

1 **Species diversity reduces risk in tropical forest restoration: a portfolio**
2 **effect across heterogeneous sites**

3

4 Rachele Quaglino^{1,φ,*}, Rebecca J. Cole^{1,2,φ}, Gerald Quirós Cedeno^{1,2}, David Rodriguez³, Jeff
5 Tingle⁴, Daniel S. Maynard⁵, Anton Weissenhofer⁶, Thomas W Crowther^{7,8}, Leland K.
6 Werden^{1,φ,*}

7 ¹Department of Environmental Systems Science, ETH Zürich, Zürich, Switzerland

8 ²Tropical Landscape and Climate Program, Agua Buena, Puntarenas Province, Costa Rica

9 ³Finca Cántaros Environmental Association, San Vito, Puntarenas Province, Costa Rica

10 ⁴Finca Aguas Buenas, Filadelfia de Buenos Aires, Puntarenas, Costa Rica

11 ⁵Department of Genetics, Evolution and Environment, University College London, London,
12 United Kingdom

13 ⁶University of Vienna, Department of Botany and Biodiversity Research, Vienna, Austria

14 ⁷BRANCH Institute, Zug, Switzerland

15 ⁸King Abdullah University of Science and Technology (KAUST), Thuwal, Saudi Arabia

16

17 *Corresponding authors: rachele2001.rq@gmail.com and lwerden@gmail.com

18 ^φAuthors contributed equally

19

20 **Keywords:** biodiversity-stability, biodiversity insurance, carbon stocks, Costa Rica, cross-
21 site buffering, multivariate dispersion, structural heterogeneity, seedling survival, tree
22 diversity experiment

23

24

25 **Running title:** Diversity reduces risk via a portfolio effect

26

27

28

29

30

31

32

33

34

35

36 **Abstract**

37 Assisted restoration is essential for recovering degraded tropical forests. Biodiversity-stability
38 theory predicts that functionally diverse communities should produce more reliable,
39 predictable outcomes than monocultures, but broad-scale field experiments in tropical
40 restoration are scarce. We established 120 plots spanning five planting treatments (two
41 monocultures – of a fast-growing nitrogen-fixer or a fleshy-fruit species – and 2-, 6-, and 12-
42 species mixes), with species selected at each richness level to maximize functional trait
43 diversity, across four sites in southwestern Costa Rica. After three years we measured height,
44 canopy cover, carbon stocks, survival, and structural heterogeneity. *Inga edulis* monocultures
45 (the same nitrogen-fixer at all four sites) achieved the highest mean carbon stocks (5.4 Mg C
46 ha⁻¹) and fastest height growth (3.7 m vs 1.7-2.2 m in mixtures) but survived less and far less
47 predictably across sites (78%, 56-100%, versus 90%, 83-95% in mixtures). Which species
48 survived consistently therefore mattered more than which grew fastest. Each site's mixtures
49 comprised different locally adapted species yet converged on consistent outcomes, so
50 predictability appeared to be a property of diverse mixtures generally, not of any single
51 shared species. Diverse mixtures were three- to four-fold less variable in survival across sites
52 and developed up to 140% more within-plot structural heterogeneity than monocultures,
53 suggesting a dual benefit of more structurally complex habitat within plots and more
54 predictable establishment across them. Because functional diversity saturated at roughly six
55 species, six-species mixes captured most of this benefit, with only marginal gains at twelve.
56 Our results provide evidence for a biodiversity portfolio effect (*i.e.*, biodiversity insurance) in
57 assisted tropical restoration, whereby functionally diverse plantings trade peak productivity
58 for predictability, buffering against the unpredictable, low-survival outcomes that drive
59 replanting costs, at little added expense.

60
61
62
63
64
65
66
67
68
69

70 **Introduction**

71 Tropical forests harbor more than half of terrestrial vertebrate species (Pillay et al.,
72 2022) and are critical for carbon sequestration, yet more than half of the world's original
73 tropical forest has been lost (Barlow et al., 2016; Lewis et al., 2015; Malhi et al., 2014). As a
74 result, natural climate solutions have emerged as a key pathway alongside fossil fuel
75 reduction to address the climate crisis (Griscom et al., 2017, 2019; Seddon et al., 2021), and
76 restoring degraded land to forests is scaling rapidly under commitments such as the Bonn
77 Challenge and the UN Decade on Ecosystem Restoration (Holl, 2017). Restoration practices
78 span a continuum from natural regeneration to assisted restoration involving direct tree
79 planting, with the latter often required in degraded landscapes where natural recovery is slow
80 (Chazdon et al., 2024; Crouzeilles et al., 2020; Stanturf, 2021). Assisted restoration is the
81 most resource-intensive approach necessary in the most degraded ecosystems, where species
82 selection is a key determinant of its outcomes (Butterfield, 1996; Fremout et al., 2021;
83 Werden et al., 2018). However, many reforestation programs prioritize fast-growing species
84 for rapid carbon sequestration, often resulting in low-diversity plantations that may
85 underperform across variable site conditions (Holl et al., 2022). As climate change intensifies
86 the unpredictability of restoration outcomes across landscapes, understanding whether species
87 diversity can buffer outcomes against site-level variation has become an urgent question for
88 both restoration science and policy, with implications for how carbon crediting programs may
89 assess permanence risk.

90 A long history of evidence from biodiversity-ecosystem functioning research suggests
91 that species diversity can enhance mean ecosystem productivity, and can also stabilize it
92 across space and time (Hector et al., 2010; Isbell et al., 2015; Loreau & De Mazancourt,
93 2013; Tilman, 1999). The biodiversity insurance hypothesis predicts that diverse
94 communities buffer ecosystem functioning against environmental variability because
95 different species respond differently, providing functional redundancy when individual
96 species underperform (Van De Peer et al., 2016; Yachi & Loreau, 1999). In this sense the
97 planting of diverse mixtures of species provides the benefits of a financial portfolio. That is,
98 by spreading investment across many species, each with a different response to local
99 conditions, it is possible to lower the risk that the whole planting underperforms, in exchange
100 for somewhat lower average early returns than the single best-performing species. Yet, until
101 now, the existence of a trade-off between stability and peak performance remains untested
102 under field conditions within a tropical restoration setting.

103 Beyond stabilizing average outcomes, species diversity in planted forests is expected
104 to increase structural heterogeneity – the variation in tree size, canopy architecture, and
105 biomass within and among plots (Holl et al., 2013; Huang et al., 2018). Structural
106 heterogeneity enhances light capture, niche partitioning, and microhabitat diversity, and is
107 increasingly recognized as a key indicator of overall performance (Baruffol et al., 2013;
108 Coverdale & Davies, 2023; Perles-Garcia et al., 2021). Broad-scale studies have generally
109 revealed a positive effect of diversity on productivity across global forests (Liang et al., 2016;
110 Zhang et al., 2012), and experimental tree diversity networks have demonstrated
111 complementarity and insurance effects in planted systems (Verheyen et al., 2016). Functional
112 diversity offers a practical framework for designing species mixes that maximize niche
113 complementarity and resource use efficiency (Cadotte et al., 2011; Díaz et al., 2007;
114 Laughlin, 2014; Ostertag et al., 2015; Petchey & Gaston, 2002). However, until now, most
115 experimental evidence for diversity-stability relationships in tree plantations comes from
116 temperate and boreal systems. Whether diversity acts as insurance for outcomes in tropical
117 restoration, where environmental heterogeneity is high and the stakes for global carbon and
118 biodiversity are greatest, remains an open question (for temperate sites *see* Van De Peer et al.,
119 2016).

120 Here, we present three-year outcomes from a tropical wet forest restoration
121 experiment spanning four degraded sites across a steep environmental gradient (450-1,160 m
122 elevation, 3,800-6,140 mm rainfall) in southwestern Costa Rica. We planted 120 plots in five
123 treatments ranging from monocultures to 12-species mixes (plus 24 unplanted controls), with
124 species selected to maximize functional trait space at each richness level. We selected species
125 at each richness level to maximize functional trait diversity from the locally available nursery
126 pool, so the richness gradient is, by design, a functional-diversity gradient. This lets us test
127 whether more functionally diverse plantings produce greater structural complexity and more
128 predictable outcomes across variable sites. We therefore read richness effects as functional-
129 diversity effects, noting the design does not isolate the two. We assessed three specific
130 questions: (1) Do fast-growing monocultures outperform diverse mixes, and does the answer
131 depend on site? (2) Through what pathways does planted diversity (functional diversity,
132 manipulated via species richness) shape within-plot structural heterogeneity? (3) Does this
133 diversity reduce cross-site variability in multivariate outcomes? We predicted that diverse
134 treatments would show lower mean productivity than the best-performing monoculture at this
135 early stage but greater consistency across sites – consistent with a portfolio effect of planting
136 functionally diverse species across a strong environmental gradient.

137 **Methods**

138 *Study sites*

139 We conducted the study at four sites, each covering 3-4 hectares, in collaboration with
140 four restoration-focused organizations: Loma Linda Field Station (LLFS), Finca Cantaros
141 Environmental Association (FCEA), Finca Aguas Buenas (FAB) and Tropical Field Station
142 La Gamba – University of Vienna (GAM). These organizations had the facilities to collect
143 seeds and grow seedlings of a wide variety of tree species native to the local area. All sites
144 were degraded lands located in tropical forest zones in southern Costa Rica, captured a range
145 of local conditions, and were widely separated (>8km), allowing us to generalize across a
146 broader region. The sites in this study are located at the boundary between the Tropical Wet
147 Forest and Premontane Wet/Rain Forest zones (Holdridge et al., 1971), range in elevation
148 from 450 to 1,160 meters, and receive an average annual rainfall of 3,800-6,140 mm, with a
149 drier season from December to March that is weak at the wettest site (La Gamba, ~6,140 mm
150 yr⁻¹). The mean annual temperature ranged from 21-28°C. All sites were used for cattle
151 grazing and mixed agriculture for >22 years (Table S1). At the start of the study, the sites
152 were primarily dominated by opportunistic non-native forage grasses including *Axonopus*
153 *scoparius*, *Pennisetum purpureum*, *Melinis minutiflora*, and *Urochloa brizantha*, along with
154 the fern *Pteridium arachnoideum*. Each site featured diverse, rugged terrain, with slopes
155 ranging from 5 to 32 degrees. The soils, of volcanic origin, were mildly acidic and low in
156 phosphorus.

157

158 *Species selection*

159 To include the broadest range of tree functional diversity in our experimental design,
160 we compiled a list of native tree species for which seedlings could be produced in sufficient
161 quantities at each site (82 species at LLFS, 56 at FCEA, 49 at FAB and 59 at GAM). We
162 standardized taxonomic names using the *Treemendous* package (Specker et al., 2024). We
163 then extracted available data from the TRY Plant Trait Database (Kattge et al., 2020) for 18
164 tree traits, including leaf (area, specific leaf area, density, thickness, nitrogen, phosphorus,
165 potassium), seed mass, bark thickness, wood density, architectural traits (maximum crown
166 height and diameter, maximum height, diameter), physiological traits (stem conduit diameter,
167 stomatal conductance, V_{cmax}), and maximum root depth (see Table S2 for full trait list and
168 units). For species with missing trait data, we imputed missing trait values using the models
169 generated in Maynard et al. (2022), which integrate phylogenetic and environmental
170 information.

171 After compiling the functional trait data, we visualized all candidate species in trait
172 space using principal components analysis (PCA). We coded categorical trait values to
173 highlight species by nitrogen-fixing status (non-fixer, nitrogen-fixer) and dispersal syndrome
174 (animal-dispersed, animal-dispersed with carbohydrate-rich fleshy fruit, other; Fig. S1). This
175 approach aligns with calls to make functional trait-based species selection more accessible to
176 restoration practitioners (Gornish et al. 2023), as tools such as the freely available Restoring
177 Ecosystem Services Tool (REST) allow users to upload a .csv file of species and trait data,
178 then perform and visualize a PCA for species selection (Rayome et al., 2019). From each
179 PCA biplot, we selected two core species based on predetermined traits: a fast-growing
180 nitrogen-fixer and a species that produces carbohydrate-rich, fleshy fruit (Table S3). We then
181 selected additional native candidate species to maximize trait diversity by filling as much trait
182 space as possible within each quadrant of the biplot, adding approximately one species per
183 quadrant to construct the 6SP treatments, then an additional six distributed across quadrants
184 to build the 12SP treatments, ensuring nursery seedling availability of each selected species.
185 Because sites were located across a diverse landscape, the selected species reflected local
186 availability and conditions. As a result, species composition (except for the *Inga edulis*
187 monoculture; M1) varied across sites, although functionally analogous species were included
188 in the same proportions across all sites (Table S3). This design created a gradient in which
189 planted species richness covaries with functional trait space occupancy, allowing us to test
190 whether greater diversity stabilized restoration outcomes across heterogeneous sites.

191

192 *Experimental design*

193 We set up the sites over a three-year period: one in 2021 (LLFS), two in 2022 (FCEA
194 and FAB) and the last in 2023 (GAM) (Fig. 1a). Each site consisted of six blocks, to account
195 for differences in microtopography, each of which contained six different tree planting
196 treatment plots ($n = 6 \text{ plots} \times 6 \text{ treatments} \times 4 \text{ sites} = 144 \text{ plots total}$) (Fig. 1b). Of these, 120
197 plots comprised the five planted treatments analyzed here, and 24 were unplanted controls
198 (not analyzed here). The treatments included: (1) a fast-growing nitrogen-fixing monoculture
199 (always *Inga edulis*; M1); (2) a monoculture of a carbohydrate-rich fruit producer (M2),
200 using a locally selected species at each site: *Ficus insipida* (FAB), *Saurauia montana*
201 (FCEA), *Citharexylum cooperi* (GAM), and *Calophyllum brasiliense* (LLFS); (3) a 50/50%
202 mix of these two core species (*i.e.*, 50% M1 species + 50% M2 species = 2SP treatment); (4)
203 a mix of the two core species plus four additional species (6-species mix); (5) a mix of the
204 same six species plus six more species (12-species mix); and, for design completeness, a sixth

205 unplanted control (natural regeneration) that we describe but did not analyze (Table 1). The
 206 unplanted control plots will be used in follow-up studies examining seed rain, seedling
 207 recruitment, and natural regeneration dynamics across the treatments. These treatments
 208 contrast restoration strategies practitioners typically use in assisted tropical forest restoration:
 209 a fast-growing nitrogen-fixer monoculture (M1, a regional default), a fleshy-fruit
 210 monoculture intended to attract seed dispersers (M2), and a 2 → 6 → 12-species richness
 211 ladder in which each level maximized functional trait diversity from the local nursery pool.
 212 All species were planted in equal amounts within each treatment plot.

213

214 **Table 1.** Details of each of the six treatments (control not analyzed). Each block has six 15 ×
 215 15m plots with one of each of the following treatments.

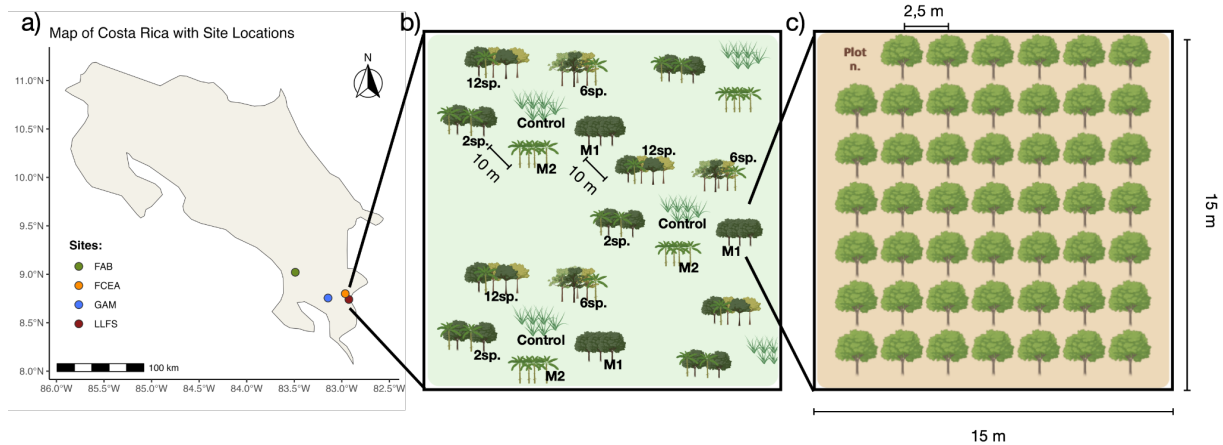
Treatment	Treatment code	Number of species planted
Control (<i>i.e.</i> , natural regeneration; not included in analysis)	C	0
Monoculture of a fast-growing nitrogen-fixer	M1	1
Monoculture of species that produces carbohydrate-rich fruit	M2	1
Nitrogen-fixer + fruit producer	2SP	2
Nitrogen-fixer + fruit producer + 4 additional species with diverse traits	6SP	6
Nitrogen-fixer + fruit producer + 4 species used above + 6 additional species with diverse traits	12SP	12

216

217 In 2021 at LLFS, 2022 at FAB and FCEA and 2023 at GAM, we established 36 plots
 218 per site, 30 of which were planted with 48 trees each (5,760 seedlings total) spaced 2.5 m
 219 apart in a grid pattern (Fig. 1c). Plots measured 15 × 15m, were spaced a minimum of 10 m
 220 apart from each other, and at least 10 m away from any other existing trees or forest edges.
 221 We distributed seedlings in the mixed-species treatments evenly across each plot following
 222 two possible designs for the 2-species mix, and four possible planting designs for the 6- and
 223 12- species mixes. We randomly assigned these designs to each plot to minimize planting
 224 location biases and ensure a fair comparison of species interactions.

225 Site preparation, tree planting and maintenance followed standard forestry practices in
 226 the region (Holl et al., 2011). We prepared the sites by clearing naturally established
 227 vegetation to ground level with machetes or string trimmers immediately prior to planting.
 228 Seedlings were planted into uniform holes (35 cm deep × 30 cm diameter) with 30 g of NPK

229 (10-30-10) fertilizer and 5 g of granular nematicide (Mocap®) mixed into the soil in the root
 230 zone. For the first year post-planting, all other vegetation within all plots (including
 231 unplanted controls) was cleared at 4-month intervals to promote seedling establishment /
 232 ensure similar initial conditions for recovery of native vegetation. During the second year,
 233 clearing was restricted to a 1-m radius around individual seedlings until they overtopped the
 234 surrounding vegetation, after which maintenance ceased. Inter-plot spaces were not cleared.
 235 Seedlings that died in the first and second year were replaced.



236

237 **Figure 1.** Experimental design in southwestern Costa Rica. (a) Geographic location of the
 238 four experimental sites. (b) At each site, six blocks each containing six randomly assigned
 239 treatment plots, spaced ≥ 10 m apart and ≥ 10 m from forest edges. (c) Each plot is 15×15 m
 240 with 48 trees spaced 2.5 m apart; control plots are unplanted.

241

242 Data collection

243 We measured planted seedling survival annually, including all replanted seedlings
 244 starting in 2022 at LLFS, 2023 at FCEA and FAB and 2024 at GAM. In February-March
 245 2024, 2025, and 2026 (3 years after planting each site), we measured height (base of trunk to
 246 apical meristem) and DBH (Diameter at Breast Height; 1.3 m) for all seedlings with a DBH \geq
 247 1 cm to quantify planted seedling performance. To simplify data collection, we measured
 248 height and DBH of a random half of monoculture seedlings (24 of 48 per plot) from 2024
 249 onward, after preliminary measurements showed highly homogeneous growth in these plots.
 250 From 2024 to 2026, we measured percent canopy cover using a spherical densiometer at 6
 251 locations within each plot.

252

253

254

255

256 **Statistical analysis**

257 Our statistical approach addressed our three questions at two levels of analysis. First,
258 we tested treatment effects on seven plot-level vegetation recovery metrics (height, canopy
259 cover, carbon, survival, and three Gini heterogeneity indices) using linear mixed-effects
260 models and used structural equation models to identify the pathways through which richness
261 shaped structural heterogeneity. Second, we assessed whether species richness stabilized
262 multivariate outcomes across sites using principal components analysis and multivariate
263 dispersion. All analyses were conducted in R v4.5.0 (R Development Core Team, 2025).

264

265 *Plot-level calculations:*

266 We calculated plot-level productivity (carbon stocks, total basal area), vegetation
267 recovery (mean height, canopy cover, survival), and structural heterogeneity (Gini
268 coefficients of height, canopy cover, and carbon) for all plots after three years of growth. We
269 estimated mean plot-level height and canopy cover as the arithmetic mean of all individuals
270 in each plot (48 individuals x plot, height) or all transects measured in each plot (6 transects x
271 plot, percent canopy cover). Then, we calculated plot-level survival as the proportion of the
272 48 planted tree positions per plot with a living individual at year 3; positions where the
273 original seedling died during years 1-2 and was successfully replanted are counted as alive,
274 consistent with our annual survival census above, which included all replanted seedlings.
275 Sensitivity analyses excluding replanted individuals from the multivariate dispersion analysis
276 are reported in Table S4.

277 We estimated aboveground biomass (AGB) using the Chave et al. (2014) pantropical
278 allometric model implemented in the BIOMASS package (Réjou-Méchain et al., 2017). We
279 assigned each species a best-estimate wood density compiled across the BIOMASS package,
280 the BIEN database (Maitner et al., 2018), the Global Wood Density Database (Chave et al.,
281 2009), the Tervuren Xylarium Wood Density Database (Verbiest et al., 2026), and the
282 CIRAD wood-density database (Vieilledent et al., 2017) using species-level values where
283 available and genus-level means for the 11 of 35 species lacking species-level data (17% of
284 biomass-measured individuals). We estimated carbon as $AGB \times 0.47$ and scaled to $Mg\ C\ ha^{-1}$.
285 We calculated total plot-level basal area by summing the basal areas of all seedlings with a
286 $DBH \geq 1$ cm within each plot at year 3 and calculated individual basal area and height of
287 *Inga edulis* per treatment at all sites to monitor monoculture species performance across
288 treatments.

289 We also calculated plot-level heterogeneity of tree height, canopy cover, and carbon
290 stocks across all planted seedlings for all assisted restoration plots (6 plots per 5 treatments
291 per site) at the end of year 3 using the Gini coefficient:

$$292 \text{ Gini coefficient} = [\sum_{i=1}^n (2i - n - 1) x_i] / (n \sum_{i=1}^n x_i)$$

293 where x_i are the values for the i -th individual (tree height, canopy cover, or carbon stocks)
294 sorted in ascending order and n is the number of individuals per plot: 48 individuals for tree
295 height and carbon Gini, and 6 densiometer transect points for canopy cover Gini.

296

297 *Comparing between treatments:*

298 We used linear mixed-effects models (*lme4* and *lmerTest*) to test how planting
299 treatments influenced plot-level outcomes. All plot-level models included treatment (5 levels:
300 M1, M2, 2SP, 6SP, 12SP), site (4 levels: FAB, FCEA, GAM, LLFS), and their interaction as
301 fixed effects, with block nested within site as a random intercept: $\text{response} \sim \text{Treatment} \times \text{Site}$
302 $+ (1|\text{Site}:\text{Block})$. We examined model assumptions using simulated residuals (*DHARMA*).
303 Where diagnostics indicated non-normality, we log-transformed responses (carbon, total
304 basal area, *Inga edulis* basal area). We modeled survival as a binomial GLMM on plot-level
305 alive/dead counts using *glmmTMB*. The survival binomial GLMM showed no significant
306 overdispersion (DHARMA test, $p = 0.12$), so we retained a binomial rather than a beta-
307 binomial. We tested the significance of fixed effects using Type-III ANOVAs with
308 Satterthwaite denominator degrees of freedom and computed partial eta-squared (η^2p) as an
309 effect size. When ANOVAs were significant, we performed pairwise treatment comparisons
310 using estimated marginal means (*emmeans*) with Tukey-adjusted p-values, and compact letter
311 displays indicated significant differences at $\alpha = 0.05$.

312 To assess whether species diversity stabilized multivariate restoration outcomes
313 across sites, we scaled the seven plot-level metrics (mean height, carbon, canopy cover,
314 survival, height Gini, canopy Gini, carbon Gini) to unit variance and performed principal
315 components analysis (PCA). We quantified how consistently each treatment performed
316 across plots and sites by measuring multivariate dispersion – the spread of plots around their
317 treatment means in seven-dimensional outcome space (betadisper; *vegan*). We first tested
318 whether monocultures and polycultures differed in multivariate dispersion using betadisper
319 with a permutation test (all five treatments included).

320 We then tested whether dispersion decreased monotonically along the designed
321 richness gradient (M1, 2SP, 6SP, 12SP). The richness gradient followed the designed
322 planting sequence; M2 tested a different species identity at richness = 1 across sites, so we

323 did not include it as part of this gradient (though we report M2-inclusive sensitivity below).
324 As our primary test of monotonic decrease, we computed the Spearman correlation between
325 richness and distance to centroid and assessed significance using a permutation test (9,999
326 permutations) with standardized effect size (SES), as permutation tests do not rely on
327 distributional assumptions that linear models on multivariate distances may violate. We
328 assessed robustness via leave-one-site-out sensitivity, exclusion of replanted individuals, and
329 a temporal trajectory across years 1–3. We also re-ran the Spearman test with M2 included
330 (coded as richness = 1 alongside M1) to confirm the dispersion–richness trend was not an
331 artifact of M2 exclusion. Because the permutation test treats plots as exchangeable, we also
332 fit a linear mixed-effects model on betadisper distances with richness as a fixed effect and
333 site and block as random intercepts, so that the richness effect is estimated while accounting
334 for the four-site structure. To check that the richness–dispersion relationship was not an
335 artifact of metrics scaling with their mean, we re-estimated it under log- and rank-
336 transformations and on a bounded-only subset (survival plus the three Gini indices) and
337 examined each metric's among-site CV and mean-variance coupling. We also computed
338 Rao's Q and functional dispersion (FDis) per treatment (*FD* package, using Gower trait
339 distances) to test whether functional diversity saturated along the richness gradient.

340 Finally, we used structural equation models (*piecewiseSEM*) to test the hypothesized
341 pathway from planted species richness through carbon accumulation and canopy cover to
342 structural heterogeneity, with site as a random effect. Again, we excluded M2 from the
343 structural equation models because it shared richness = 1 with M1 but differed in species
344 identity across sites; as a reparameterization check, a supplementary structural equation
345 model recoded the gradient as *I. edulis* proportion (collinear with richness) and included all
346 treatments.

347

348 **Results**

349 We present results pooled across all four sites. Site-specific results, model
350 diagnostics, and robustness analyses are in the supplement (Figs. S2-S12, Tables S4-S8).

351

352 *Plot-level ecosystem outcomes:*

353 Planted species richness strongly influenced plot-level ecosystem outcomes after three
354 years (Table 2; Fig. 2). Mean tree height differed significantly among treatments ($F_{4,79} =$
355 46.34, $p < 0.001$, $\eta^2p = 0.70$), with *I. edulis* monocultures (M1) reaching 3.70 ± 1.06 m
356 compared to 1.66-2.20 m in mixed-species treatments and 1.29 m in M2. Canopy cover

357 followed a similar pattern ($F_{4,79} = 29.35$, $p < 0.001$, $\eta^2p = 0.60$), with M1 averaging 71%
358 versus 23-42% in mixed treatments and 11% in M2. Estimated carbon stocks were highest in
359 M1 (5.44 ± 4.06 Mg C ha⁻¹) and lowest in M2 (0.09 Mg C ha⁻¹), with 2SP-12SP treatments
360 intermediate at 1.76-2.60 Mg C ha⁻¹ ($F_{4,75.5} = 44.84$, $p < 0.001$, $\eta^2p = 0.70$). The Treatment \times
361 Site interaction was significant for carbon ($p = 0.045$), reflecting M1's variable performance
362 across sites (*see* Figs. S3-S6).

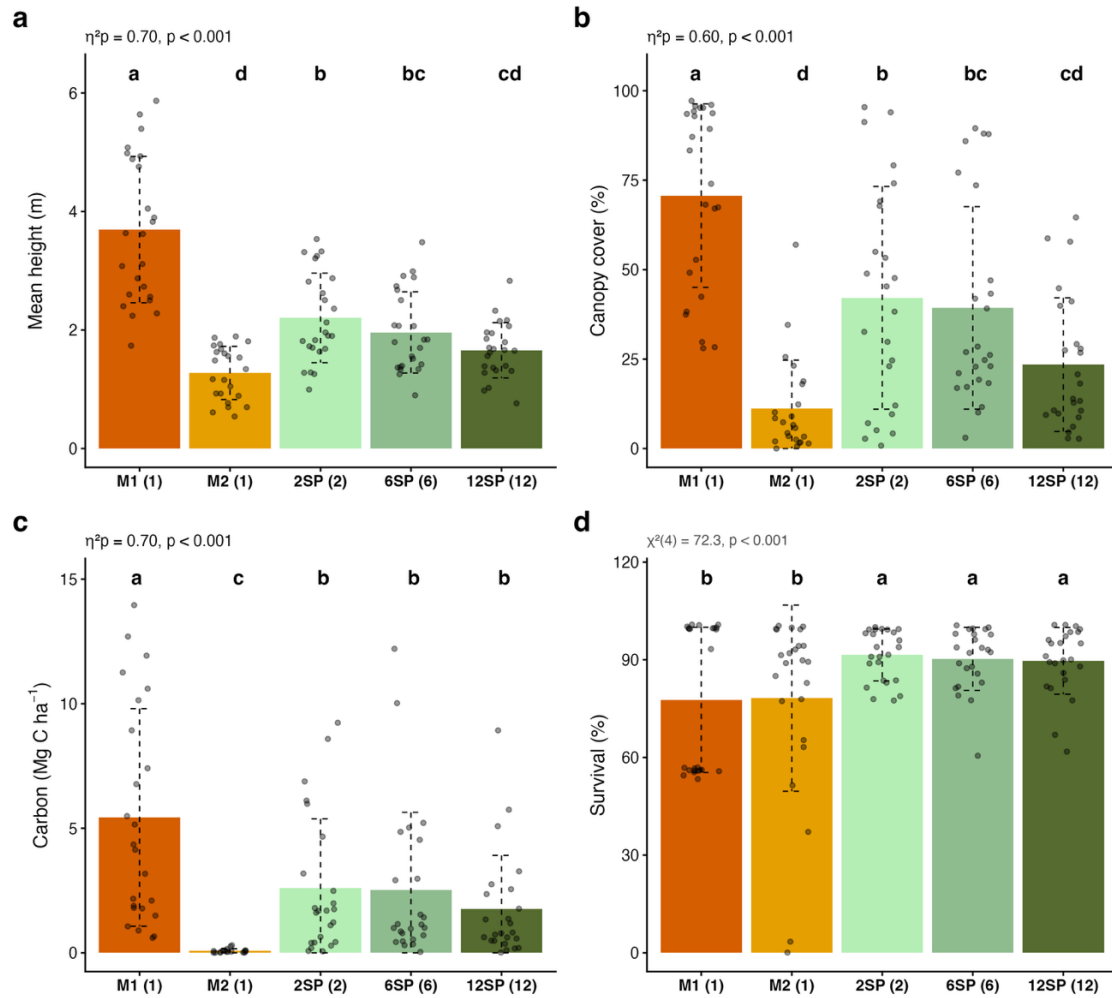
363 Survival differed among treatments (Wald $\chi^2 = 72.3$, $df = 4$, $p < 0.001$) with a strong
364 Treatment \times Site interaction (Wald $\chi^2 = 165.9$, $df = 12$, $p < 0.001$). Mixed-species treatments
365 averaged 90% survival (83–95% across sites) and performed similarly across the three
366 richness levels (each ~90–91%), while both monocultures were lower and more variable: M1
367 averaged 78% but ranged from 56% at FCEA and LLFS to 99-100% at FAB and GAM, and
368 M2 averaged 78% but with high among-plot variability (SD = 26%).

369

370 *Structural heterogeneity:*

371 Within-plot structural heterogeneity, measured with the Gini coefficient, increased
372 with planted species richness for all three metrics (Fig. 3). Height heterogeneity showed the
373 strongest treatment effect ($F_{4,79.2} = 135.82$, $p < 0.001$, $\eta^2p = 0.87$), increasing 140% – from
374 0.16 in M1 to 0.39 in 12-species plots – with a significant Treatment \times Site interaction
375 ($F_{12,79.2} = 5.23$, $p < 0.001$). Canopy cover heterogeneity followed a similar gradient ($F_{4,77.9} =$
376 24.57, $p < 0.001$, $\eta^2p = 0.56$), though M2 was an outlier with the highest values (0.49) due to
377 patchy seedling mortality. Carbon stock heterogeneity likewise increased with richness
378 ($F_{4,76.1} = 37.73$, $p < 0.001$, $\eta^2p = 0.67$), from 0.28 in M2 and 0.43 in M1 to 0.62 in 12-species
379 plots, reflecting the combined effects of species mixes on wood density and growth rates.

380



381

382 **Figure 2.** Ecosystem outcomes across planting treatments pooled across four sites after three
 383 years. (a) Mean tree height, (b) canopy cover, (c) carbon stocks, and (d) survival. Bars are
 384 treatment means \pm standard errors. Letters denote significant pairwise differences (Tukey
 385 HSD for panels a-c; Sidak-adjusted for panel d; $p < 0.05$); η^2p from linear mixed models with
 386 block nested within site as a random effect. M1 = *Inga edulis* monoculture, M2 = fleshy-fruit
 387 monoculture, 2SP/6SP/12SP = 2-, 6-, and 12-species mixes.

388

389

390

391

392

393

394

395

396

397

398

399

400

401

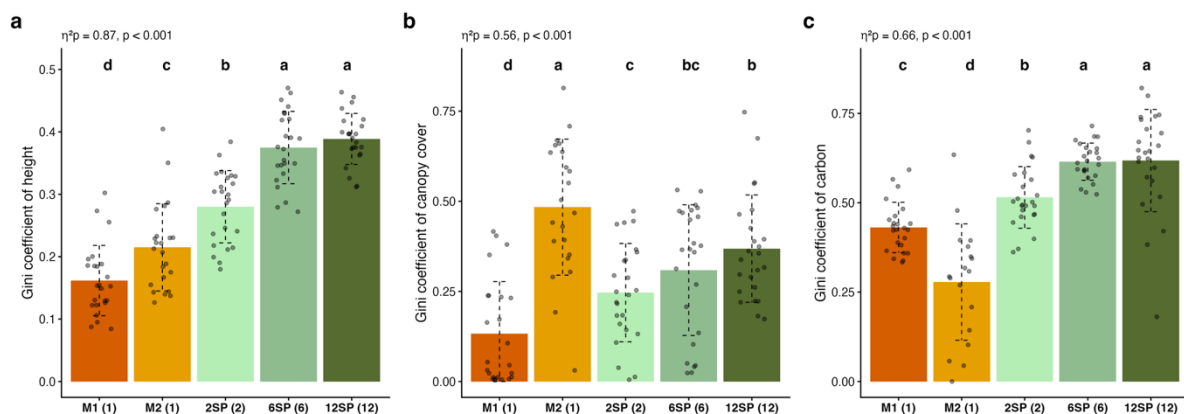
402

403

404 **Table 2.** Results of linear mixed-effects models for seven plot-level ecosystem outcomes,
 405 with treatment, site, and their interaction as fixed effects and block nested within site as a
 406 random intercept. F-values, numerator (df_1) and denominator (df_2) degrees of freedom, p-
 407 values, and partial eta-squared (η^2p) shown for each fixed effect. Denominator degrees of
 408 freedom estimated via Satterthwaite approximation. Survival modeled as a binomial GLMM.
 409 Survival rows report Wald χ^2 (df shown), not F.
 410

Metric	Term	F	df_1	df_2	p-value	η^2p
Mean height (m)	Treatment	46.34	4	79.0	< 0.001	0.70
	Site	12.28	3	19.7	< 0.001	0.65
	Treatment \times Site	1.13	12	79.0	0.346	0.15
Canopy cover (%)	Treatment	29.35	4	79.0	< 0.001	0.60
	Site	7.62	3	19.8	0.001	0.54
	Treatment \times Site	1.51	12	79.0	0.139	0.19
Carbon (Mg C ha ⁻¹)	Treatment	44.84	4	75.5	< 0.001	0.70
	Site	5.55	3	20.4	0.006	0.45
	Treatment \times Site	1.92	12	75.3	0.045	0.23
Height Gini	Treatment	135.82	4	79.2	< 0.001	0.87
	Site	8.03	3	19.9	0.001	0.55
	Treatment \times Site	5.23	12	79.2	< 0.001	0.44
Canopy Gini	Treatment	24.57	4	77.9	< 0.001	0.56
	Site	10.23	3	19.3	< 0.001	0.61
	Treatment \times Site	1.86	12	77.8	0.052	0.22
Carbon Gini	Treatment	37.73	4	76.1	< 0.001	0.67
	Site	1.81	3	20.7	0.176	0.21
	Treatment \times Site	1.35	12	75.9	0.209	0.18
Survival (%)	Treatment	72.33	4	-	< 0.001	-
	Site	45.82	3	-	< 0.001	-
	Treatment \times Site	165.9	12	-	< 0.001	-

411



412

413 **Figure 3.** Within-plot structural heterogeneity (Gini coefficient) for (a) tree height, (b)
 414 canopy cover, and (c) carbon stocks after three years. Higher values indicate greater within-
 415 plot inequality. Bars are treatment means \pm standard errors. Letters denote significant
 416 pairwise differences (Tukey HSD, $p < 0.05$); η^2p from linear mixed models with block nested
 417 within site as a random effect.

418 *Multivariate synthesis and diversity-stability:*

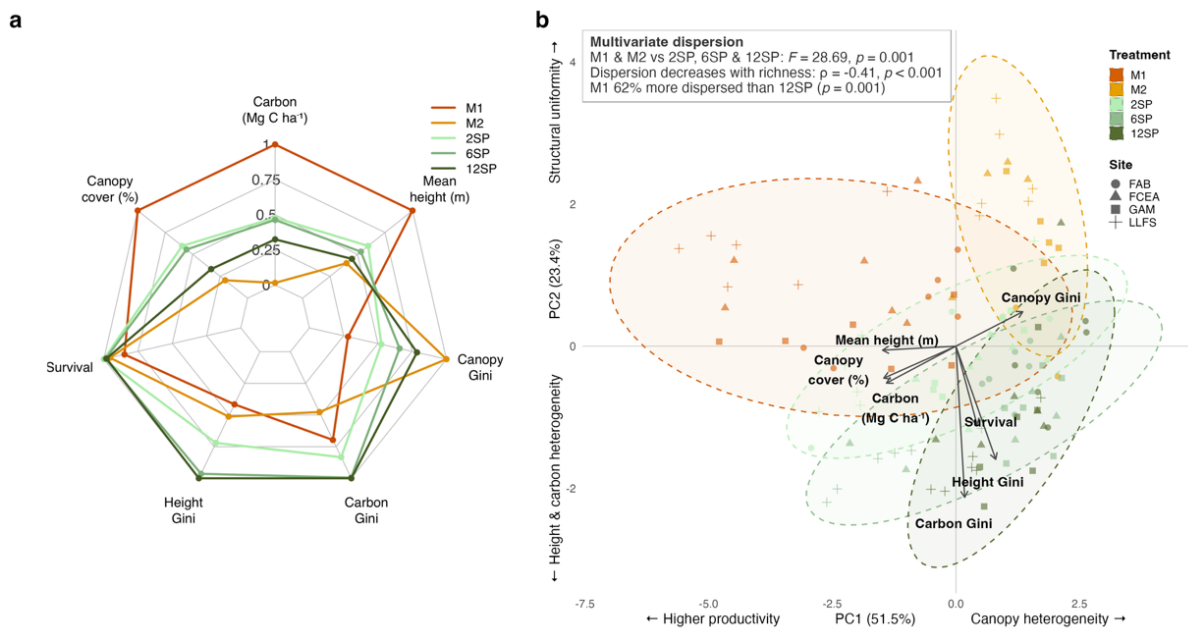
419 A principal components analysis of the seven plot-level metrics (Fig. 4b) showed
420 clear separation of treatments in multivariate space. PC1 (51.5%) separated monocultures
421 from mixed treatments along a gradient from higher productivity (height, carbon, canopy
422 cover) to greater canopy heterogeneity. PC2 (23.4%) captured a gradient from structural
423 uniformity (monocultures) to height and carbon heterogeneity, with survival loading in the
424 same direction as the Gini indices. Notably, the 95% confidence ellipses for M1 were visibly
425 larger than those for diverse treatments, a pattern quantified by the betadisper analysis below,
426 indicating greater multivariate variability across sites. Monocultures were significantly more
427 dispersed than mixed-species treatments in multivariate outcome space (permutest $F = 28.69$,
428 $p = 0.001$; all five treatments included). This difference was concentrated in the fast-growing
429 *I. edulis* monoculture (M1), which was significantly more dispersed than every other
430 treatment, including the fleshy-fruit monoculture (all pairwise $p \leq 0.004$; Table S4C); no
431 other pair differed ($p \geq 0.37$).

432 Along the designed richness gradient (M1, 2SP, 6SP, 12SP), outcomes became more
433 consistent across sites as planted richness increased (all seven-metric dispersion: Spearman ρ
434 $= -0.41$, permutation $p < 0.001$, Table S4A, Fig. 4b; mixed-effects model accounting for site:
435 $\beta = -0.061$, $p < 0.001$, Table S4B). This did not appear to be an artifact of the productivity
436 metrics' high values: the trend was as strong when restricted to only the bounded survival and
437 structural-heterogeneity metrics, which could not be inflated by high means ($\rho = -0.41$, $p <$
438 0.001 ; Table S5). This pattern was strongest when examining only survival, the one outcome
439 immune to mean-variance scaling, and most variable across monocultures (survival-only $\rho =$
440 -0.52 , $p < 0.001$). This composite dispersion trend was partly an artifact of scale. It weakened
441 when the metrics were rank-transformed, because the productivity metrics' among-site
442 variability tracked their means rather than falling with richness. The cross-site predictability
443 benefit therefore rested primarily on the bounded survival and structural outcomes (Table
444 S5). Six-species plots captured most of this benefit, with only marginal further gains at
445 twelve. This saturation was confirmed by the trait data, as functional diversity (Rao's Q) rose
446 from monocultures through two- and six-species mixes (~ 0.035 and 0.070 , respectively), but
447 only $\sim 4\%$ further to twelve species (Table S6, Fig. S12), with the six additional species
448 adding little functional diversity across all sites.

449 This result was robust to the removal of any single site (leave-one-site-out: $\rho = -0.48$,
450 $p < 0.001$ without FAB; $\rho = -0.33$, $p = 0.004$ without FCEA; $\rho = -0.35$, $p = 0.003$ without
451 GAM; $\rho = -0.30$, $p = 0.010$ without LLFS; Table S4D), to exclusion of replanted individuals

452 ($\rho = -0.37$, $p = 0.0002$; 8.1% of trees; Table S4E), and to log-transformed richness ($p <$
 453 0.001). Including M2 in the richness gradient confirmed the pattern ($\rho = -0.31$, $p = 0.001$).
 454 The trend direction was consistent across measurement years, strengthening from year 2 ($\rho =$
 455 -0.20 , $p = 0.088$) to year 3 ($\rho = -0.38$, $p = 0.001$) in the three-site temporal subset (Table
 456 S4F). Partitioning this dispersion into among- and within-site components showed that
 457 planted richness reduced variability at both scales (Table S4G). The probability that a stand
 458 fell below 70% survival declined from 23% in monocultures to 2.5% in 12-species mixtures
 459 (odds ratio 0.80 per added species, $p = 0.02$; Table S7).

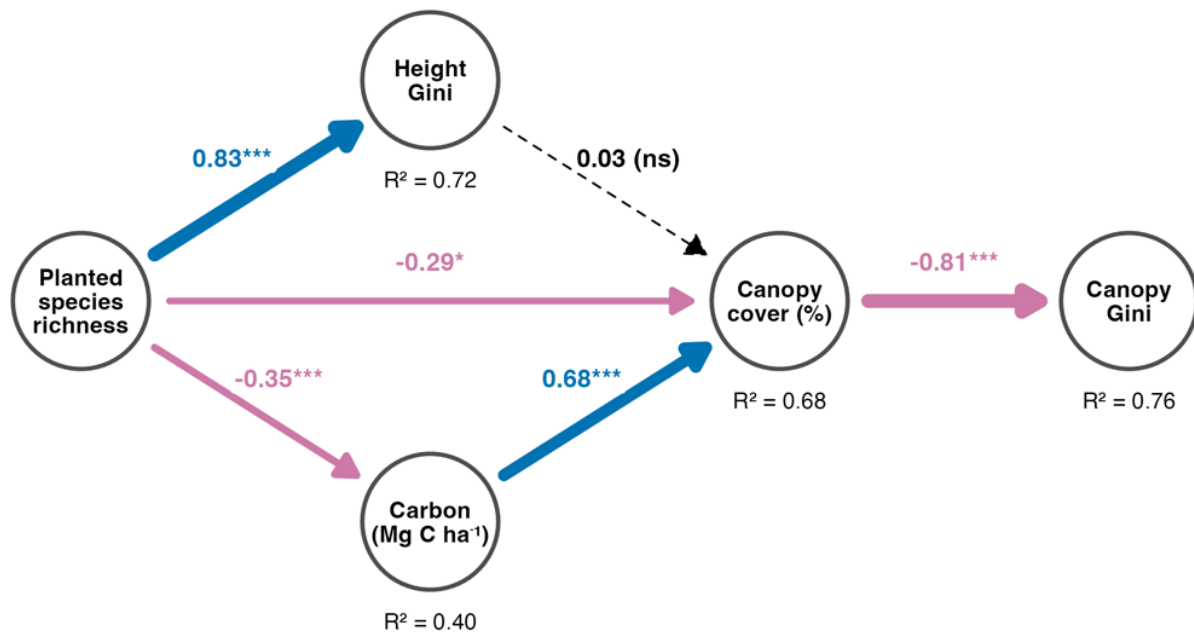
460 The normalized radar plot (Fig. 4a) illustrates treatment profiles across all seven
 461 metrics, with M1 dominating productivity-related axes but scoring lowest on heterogeneity.
 462 Although M1 held the highest mean carbon, it accumulated the most at its two lowest-
 463 survival sites (8.28 Mg C ha⁻¹ at LLFS, 4.74 at FCEA, both ~56% survival), decoupling
 464 carbon from establishment success. At the individual scale, *I. edulis* basal area averaged 28%
 465 higher in 12-species plots than in monoculture, overyielding at three of four sites (Fig. S10).



466
 467 **Figure 4.** Multivariate synthesis of treatment outcomes. (a) Radar plot of seven plot-level
 468 metrics averaged by treatment, normalized to each metric's maximum (1.0 = highest-
 469 performing treatment). (b) Principal components analysis of the same metrics with 95%
 470 confidence ellipses; PC1 (51.5%) separates monocultures from diverse treatments along
 471 productivity and survival, PC2 (23.4%) captures structural heterogeneity. Cross-site
 472 consistency increased with planted richness (seven-metric dispersion $\rho = -0.41$, $p < 0.001$),
 473 most robustly in the bounded survival and structural outcomes (survival-only $\rho = -0.52$; Table
 474 S5). M2 (fleshy-fruit monoculture) is shown but excluded from the dispersion–richness
 475 correlation as a different species identity at richness = 1 rather than a point on the designed
 476 gradient (M2-inclusive $\rho = -0.31$, $p = 0.001$).
 477

478 *Structural equation model:*

479 The piecewise structural equation model (excluding M2; Fisher's C = 8.55, df = 6, p =
 480 0.20) revealed that planted species richness was associated with structural heterogeneity
 481 through two pathways (Fig. 5). Richness showed a strong positive association with height
 482 heterogeneity ($\beta = 0.83$, $p < 0.001$) and a negative effect on carbon accumulation ($\beta = -0.35$,
 483 $p < 0.001$). Carbon in turn had a strong positive effect on canopy cover ($\beta = 0.68$, $p < 0.001$),
 484 while canopy cover strongly reduced canopy heterogeneity ($\beta = -0.81$, $p < 0.001$). The direct
 485 effect of richness on canopy cover was negative ($\beta = -0.29$, $p < 0.05$), and the path from
 486 height heterogeneity to canopy cover was non-significant ($\beta = 0.03$, ns). Marginal R² values
 487 (fixed effects only) were 0.68 (height Gini), 0.11 (carbon), 0.67 (canopy cover), and 0.75
 488 (canopy Gini); conditional R² values (including site random effect) were 0.72, 0.40, 0.68, and
 489 0.76 respectively. A supplementary structural equation model using *I. edulis* proportion as the
 490 predictor (all treatments included) recovered the same pathways (Fig. S11, Table S8).
 491 Individual-level performance of *Inga edulis* across treatments is reported in Fig. S10.



492

493 **Figure 5.** Piecewise structural equation model of pathways from planted species richness
 494 (log-transformed) to ecosystem outcomes (M2 excluded; Fisher's C = 8.55, p = 0.20). Arrow
 495 widths proportional to standardized path coefficients (β); blue arrows indicate positive
 496 effects, pink arrows negative effects. Solid arrows significant ($p < 0.05$), dashed arrows non-
 497 significant. The non-significant direct path from richness to canopy Gini ($\beta = 0.08$, $p = 0.19$)
 498 is omitted for clarity (Table S8). R² values are conditional (including site random effect).
 499

500

501

502 Discussion

503 We found a dual benefit of increased planted species richness in assisted tropical
504 forest restoration. (1) Within plots, structural heterogeneity rose sharply (height Gini: 0.16 in
505 monocultures to 0.39 in 12-species plots; a 140% increase and the strongest treatment effect
506 of any metric). (2) Across sites, multivariate outcome variability fell, most clearly in survival,
507 which varied three- to four-fold more across sites in monocultures than in diverse mixtures.
508 This combination of effects means more complex forests can provide more predictable
509 outcomes across landscapes, with direct implications for how we design restoration plantings
510 to maximize success. Notably, our diverse treatments used different locally adapted species at
511 each site yet showed similarly low multivariate dispersion (M2-inclusive $\rho = -0.31$, $p =$
512 0.001), so the stabilization appeared to reflect functional diversity rather than any single
513 shared species composition. This mean-variance trade-off mirrors classic portfolio theory
514 (e.g., Schindler et al., 2015) and provides early multi-site experimental evidence for
515 portfolio-like cross-site buffering with increasing species diversity in tropical forest
516 restoration (Yachi & Loreau, 1999).

517 The biodiversity insurance hypothesis predicts that diverse communities buffer
518 ecosystem functioning against environmental variation through response diversity, the
519 differential responses of species to local conditions (Elmqvist et al., 2003; Yachi & Loreau,
520 1999). Our results appeared consistent with this prediction. This buffering may represent the
521 assisted restoration corollary of the insurance effect that functional diversity confers on forest
522 functioning under fluctuating conditions (Chen et al., 2025). This insurance effect was
523 clearest for survival and structural outcomes, and is the spatial counterpart of the temporal
524 stability of productivity that tree diversity confers at the long-running Sardinilla experiment
525 (Schnabel et al., 2019), and is consistent with the positive effects of tree diversity on tropical
526 restoration documented in Sabah (Veryard et al., 2023). With only four sites we could not
527 cleanly separate a pure among-site (spatial) insurance effect from greater within-site
528 consistency, and co-occurring species shared local conditions that would limit independent
529 responses; variance partitioning (Table S4G) indicated that diversity reduced variability at
530 both scales, so we interpreted the result as portfolio-like buffering rather than spatial
531 insurance in the strict sense. Prior work has shown tree diversity stabilizing individual
532 outcomes, most notably reduced variability in sapling survival under drought across 34
533 TreeDivNet experiments (Blondeel et al., 2024), but primarily in temperate systems. Our
534 study builds on this evidence by evaluating the recovery of multiple ecosystem metrics

535 simultaneously, and assessing predictability across heterogeneous sites rather than through
536 time (Depauw et al., 2024; Liu et al., 2026).

537 Species richness also appeared to increase within-plot structural heterogeneity, and
538 the structural equation model linked richness to heterogeneity through two pathways: a direct
539 positive effect on height diversity ($\beta = 0.83$), and an indirect negative pathway through
540 carbon accumulation and canopy cover (richness to carbon $\beta = -0.35$, carbon to canopy cover
541 $\beta = 0.68$, canopy cover to canopy heterogeneity $\beta = -0.81$). These pathways appeared to trade
542 off. Fast-growing *Inga edulis* monocultures closed the canopy quickly but with a structurally
543 uniform overstory typical of species-poor tropical plantations (Menalled et al., 1998), and
544 their high carbon was concentrated in a thinned cohort of larger survivors. Diverse treatments
545 instead developed more heterogeneous, multi-layered canopies with gaps, which as these
546 forests mature may create a wider range of light environments and facilitate recruitment of
547 shade-tolerant species (Bullock et al., 2022; Coverdale & Davies, 2023; Holl et al., 2013).
548 Whether this structural advantage translates into greater natural recruitment remained a key
549 question for continued monitoring.

550 The site-dependent performance of *I. edulis* appeared to make the risk-management
551 case concrete. In monocultures it reached 99-100% survival at FAB and GAM but just 56%
552 at FCEA and LLFS, likely driven by density-dependent competition in pure stands.
553 Embedded in diverse mixes, its individual basal area matched or exceeded monoculture
554 values – averaging 28% higher in 12-species plots and overyielding at three of four sites –
555 consistent with reduced intraspecific competition and the complementarity effects reported in
556 other biodiversity-ecosystem functioning experiments (Huang et al., 2018; Schnabel et al.,
557 2019). More broadly, which species established reliably appeared to matter more than which
558 maximized mean performance: *I. edulis* monocultures had the highest carbon at all four sites
559 but the lowest, most variable survival (78%, 56-100%), whereas mixed treatments maintained
560 more consistently high survival (90%, 83-95%). Although the monoculture accumulated
561 more carbon at this early stage, mixed plantings tend to overtake monocultures in carbon over
562 time (Schnabel et al., 2025; Warner et al., 2023). Six-species mixes captured most of the
563 stabilizing benefit (31% dispersion reduction from monocultures, only 7% more at 12
564 species), suggesting that roughly six functionally complementary species may suffice where
565 sourcing many is logistically difficult.

566 The cost of this insurance appeared modest. Assisted tree planting in Latin America
567 costs ~US\$3,000/ha through establishment (Brancalion et al., 2019; Cole et al., 2024), and
568 because trees planted per hectare are fixed regardless of species count, diversifying adds only

569 the logistical cost of sourcing multiple natives, not a financial one. For that low marginal
570 cost, mixtures established more reliably (~90% vs 78% survival) and varied less across sites
571 ($p = -0.41$), lowering the risk of the most expensive outcome: replanting after low survival.
572 This ecological portfolio effect may have an economic parallel in the same country: across
573 two northern Costa Rican sites, mixed-species plantations outperformed monocultures by up
574 to US\$3,135/ha in timber net present value (and US\$3,500–16,800/ha once carbon credits
575 were included), with the advantage greatest when evaluated from the planting decision a
576 practitioner faces before outcomes are known (Pinnschmidt et al., 2023). This benefit was
577 one of establishment reliability rather than carbon: *I. edulis* had both the highest mean carbon
578 (5.4 Mg C ha^{-1}) and the lowest carbon CV (~80% vs 107-124% for mixes), so judged on
579 carbon accumulation alone the monoculture remained the stronger early choice. Whether
580 diversity also lowers the longer-term carbon risk that buffer pools are designed to cover –
581 reversal under drought, pests, or disturbance, against which standards such as Verra and Gold
582 Standard withhold credits (Anderegg et al., 2020, 2025) – is plausible but needs further
583 investigation. Diverse stands also spread carbon across more stems and species, whereas the
584 monoculture concentrated it in a few large individuals, so we framed any buffer-deduction
585 benefit as a hypothesis our results motivate but cannot yet confirm. This portfolio argument
586 may add a practical risk-management dimension to existing ecological rationales for diverse
587 plantings (Biggs et al., 2020; Paterno et al., 2024).

588 A deeper question is whether practitioners could predict in advance which
589 monoculture would perform reliably, and our experiment suggested they could not. *I. edulis*
590 was chosen for its strong regional track record yet established poorly at two sites, and the
591 fleshy-fruit monocultures (M2) established poorly everywhere ($0.09 \text{ Mg C ha}^{-1}$).
592 Diversification appeared to hedge against this unpredictability whether the mechanism was
593 statistical averaging, complementarity, or dilution of a volatile species (a SEM recoded with
594 *I. edulis* proportion recovered the same pathways; Fig. S11). The result's reach is nonetheless
595 bounded. Richness covaried with functional diversity by design, species were selected to
596 maximize trait space at each level, as practitioners would, so we could not separate the two,
597 and the stabilization was most plausibly a functional-diversity effect that functionally
598 redundant mixes would be expected to lack. Additionally, the analysis spanned only four sites
599 with contrasting land-use histories and only the first three years of establishment, the window
600 when most mortality occurs in tropical tree plantings (Charles et al., 2018; Werden et al.,
601 2018), so the effect should be tested across larger networks as tropical tree diversity
602 experiments mature. Reliable early establishment may nonetheless be a precondition for the

603 diversity-productivity gains that tend to strengthen with stand age (e.g., Bongers et al., 2021;
604 Liu et al., 2026), so the buffering we observed could compound rather than decline over time.

605 These results may have direct implications for restoration under climate change. If
606 diversity buffers outcomes across our current spatial environmental gradient (450-1,160 m
607 elevation, 3,800-6,140 mm rainfall), it may also buffer against the temporal shifts climate
608 change will impose on individual sites, a hypothesis that would warrant longer-term
609 monitoring, as plantings established today face changing temperature, precipitation, and
610 novel pest and pathogen pressures (Malhi et al., 2014). Our evidence is consistent across four
611 sites tracked simultaneously, but extending it to temporal buffering of climate change at a
612 single site remains untested, a question that only longer-term monitoring can examine.
613 Because carbon crediting and ecosystem-service programs depend on predictable, long-term
614 outcomes (Anderegg et al., 2020), a monoculture that establishes unreliably across sites
615 would undermine that predictability, making robustness to environmental variability a
616 financial as well as an ecological question.

617 To meet global restoration commitments, the question of which species to plant has
618 become increasingly consequential. Our results show that monocultures of fast-growing
619 species can maximize carbon at individual sites, but they can also underperform at others. In
620 contrast, diverse plantings deliver more consistent and predictable outcomes, particularly
621 across the heterogeneous landscapes where restoration is most needed. Given the
622 considerable financial risks undertaken by forest restoration practitioners across the globe,
623 our results highlight that species diversity can provide a vital level of insurance, assembling a
624 portfolio that trades peak performance for reliability. Across variable conditions, designing
625 diverse, trait-complementary species mixes that perform reliably is not just ecologically
626 sound but essential for meeting landscape-level recovery goals.

627

628 **Acknowledgments**

629 Funding was provided by a donation to the Tropical Landscape and Climate Program (LKW,
630 RJC), the Las Hermanas Carpenter Scholarship Program (GQC), and a World Economic
631 Forum grant (TWC). We thank J. Seigel as well as J. Castro, R. Gomez, F. Gomez, M.
632 Castillo, S. Gomez Villa, and J. Cruz of the Loma Linda Field Station for field assistance. All
633 research complied with applicable laws in Costa Rica.

634

635

636

637 **CRedit author contributions**

638 *Conceptualization:* RJC, LKW. *Methodology:* RJC, DM, LKW, TWC. *Formal analysis:* RQ,
639 LKW. *Investigation:* RJC, GQC, LKW, DR, JT, AW. *Data curation:* RQ, RJC, LKW.

640 *Writing - original draft:* RQ, LKW, RJC. *Writing - review and editing:* all authors.

641 *Visualization:* RQ, LKW. *Supervision:* RJC, LKW. *Funding acquisition:* RJC, LKW, TWC.

642

643 **Conflict of interest**

644 LKW is a pro-bono scientific advisor to Plant-for-the-Planet Foundation and Green Again
645 Madagascar, non-profit organizations implementing tropical restoration. RJC is the founder
646 of the non-profit Tropical Landscape and Climate Program, where LKW is a pro-bono board
647 member. TWC is the founder of the non-profit Restor Eco AG and serves on the Foundation
648 board in a pro bono capacity.

649

650 **Data and code availability statement**

651 All data and code required to reproduce the analysis are openly available in FxnDiv-
652 restoration-portfolio at <https://zenodo.org/records/20942837>.

653

654 **References**

655 Anderegg, W. R. L., Trugman, A. T., Badgley, G., Anderson, C. M., Bartuska, A., Ciais, P.,

656 Cullenward, D., Field, C. B., Freeman, J., Goetz, S. J., Hicke, J. A., Huntzinger, D.,

657 Jackson, R. B., Nickerson, J., Pacala, S., & Randerson, J. T. (2020). Climate-driven

658 risks to the climate mitigation potential of forests. *Science*, 368(6497), eaaz7005.

659 <https://doi.org/10.1126/science.aaz7005>

660 Anderegg, W. R. L., Trugman, A. T., Vargas G., G., Wu, C., & Yang, L. (2025). Current

661 Forest Carbon Offset Buffer Pool Contributions Do Not Adequately Insure Against

662 Disturbance-Driven Carbon Losses. *Global Change Biology*, 31(6), e70251.

663 <https://doi.org/10.1111/gcb.70251>

664 Barlow, J., Lennox, G. D., Ferreira, J., Berenguer, E., Lees, A. C., Nally, R. M., Thomson, J.

665 R., Ferraz, S. F. D. B., Louzada, J., Oliveira, V. H. F., Parry, L., Ribeiro De Castro

666 Solar, R., Vieira, I. C. G., Aragão, L. E. O. C., Begotti, R. A., Braga, R. F., Cardoso,

667 T. M., De Oliveira, R. C., Souza Jr, C. M., ... Gardner, T. A. (2016). Anthropogenic
668 disturbance in tropical forests can double biodiversity loss from deforestation. *Nature*,
669 535(7610), 144–147. <https://doi.org/10.1038/nature18326>

670 Baruffol, M., Schmid, B., Bruelheide, H., Chi, X., Hector, A., Ma, K., Michalski, S., Tang,
671 Z., & Niklaus, P. A. (2013). Correction: Biodiversity Promotes Tree Growth during
672 Succession in Subtropical Forest. *PLoS ONE*, 8(12).
673 <https://doi.org/10.1371/annotation/48869dee-d4a9-4ff5-a401-ce73440e7ecf>

674 Biggs, C. R., Yeager, L. A., Bolser, D. G., Bonsell, C., Dichiera, A. M., Hou, Z., Keyser, S.
675 R., Khursigara, A. J., Lu, K., Muth, A. F., Negrete, B., & Erisman, B. E. (2020). Does
676 functional redundancy affect ecological stability and resilience? A review and meta-
677 analysis. *Ecosphere*, 11(7), e03184. <https://doi.org/10.1002/ecs2.3184>

678 Blondeel, H., Guillemot, J., Martin-StPaul, N., Druel, A., Bilodeau-Gauthier, S., Bauhus, J.,
679 Grossiord, C., Hector, A., Jactel, H., Jensen, J., Messier, C., Muys, B., Serrano-León,
680 H., Auge, H., Barsoum, N., Birhane, E., Bruelheide, H., Cavender-Bares, J., Chu, C.,
681 ... Baeten, L. (2024). Tree diversity reduces variability in sapling survival under
682 drought. *Journal of Ecology*, 112(5), 1164–1180. [https://doi.org/10.1111/1365-](https://doi.org/10.1111/1365-2745.14294)
683 [2745.14294](https://doi.org/10.1111/1365-2745.14294)

684 Bongers, F. J., Schmid, B., Bruelheide, H., Bongers, F., Li, S., Von Oheimb, G., Li, Y.,
685 Cheng, A., Ma, K., & Liu, X. (2021). Functional diversity effects on productivity
686 increase with age in a forest biodiversity experiment. *Nature Ecology & Evolution*,
687 5(12), 1594–1603. <https://doi.org/10.1038/s41559-021-01564-3>

688 Brancalion, P. H. S., Meli, P., Tymus, J. R. C., Lenti, F. E. B., M. Benini, R., Silva, A. P. M.,
689 Isernhagen, I., & Holl, K. D. (2019). What makes ecosystem restoration expensive? A
690 systematic cost assessment of projects in Brazil. *Biological Conservation*, 240,
691 108274. <https://doi.org/10.1016/j.biocon.2019.108274>

692 Bullock, J. M., Fuentes-Montemayor, E., McCarthy, B., Park, K., Hails, R. S., Woodcock, B.
693 A., Watts, K., Corstanje, R., & Harris, J. (2022). Future restoration should enhance
694 ecological complexity and emergent properties at multiple scales. *Ecography*,
695 2022(4), ecog.05780. <https://doi.org/10.1111/ecog.05780>

696 Butterfield, R. P. (1996). Early species selection for tropical reforestation: A consideration of
697 stability. *Forest Ecology and Management*, 81(1–3), 161–168.
698 [https://doi.org/10.1016/0378-1127\(95\)03649-0](https://doi.org/10.1016/0378-1127(95)03649-0)

699 Cadotte, M. W., Carscadden, K., & Mirotchnick, N. (2011). Beyond species: Functional
700 diversity and the maintenance of ecological processes and services: Functional
701 diversity in ecology and conservation. *Journal of Applied Ecology*, 48(5), 1079–1087.
702 <https://doi.org/10.1111/j.1365-2664.2011.02048.x>

703 Charles, L. S., Dwyer, J. M., Smith, T. J., Connors, S., Marschner, P., & Mayfield, M. M.
704 (2018). Species wood density and the location of planted seedlings drive early-stage
705 seedling survival during tropical forest restoration. *Journal of Applied Ecology*, 55(2),
706 1009–1018. <https://doi.org/10.1111/1365-2664.13031>

707 Chave, J., Coomes, D., Jansen, S., Lewis, S. L., Swenson, N. G., & Zanne, A. E. (2009).
708 Towards a worldwide wood economics spectrum. *Ecology Letters*, 12(4), 351–366.
709 <https://doi.org/10.1111/j.1461-0248.2009.01285.x>

710 Chave, J., Réjou-Méchain, M., Búrquez, A., Chidumayo, E., Colgan, M. S., Delitti, W. B. C.,
711 Duque, A., Eid, T., Fearnside, P. M., Goodman, R. C., Henry, M., Martínez-Yrizar,
712 A., Mugasha, W. A., Muller-Landau, H. C., Mencuccini, M., Nelson, B. W.,
713 Ngomanda, A., Nogueira, E. M., Ortiz-Malavassi, E., ... Vieilledent, G. (2014).
714 Improved allometric models to estimate the aboveground biomass of tropical trees.
715 *Global Change Biology*, 20(10), 3177–3190. <https://doi.org/10.1111/gcb.12629>

716 Chazdon, R. L., Falk, D. A., Banin, L. F., Wagner, M., J. Wilson, S., Grabowski, R. C., &
717 Suding, K. N. (2024). The intervention continuum in restoration ecology: Rethinking
718 the active–passive dichotomy. *Restoration Ecology*, 32(8), e13535.
719 <https://doi.org/10.1111/rec.13535>

720 Chen, C., Bongers, F. J., Schmid, B., Ma, K., & Liu, X. (2025). Ecosystem consequences of
721 functional diversity in forests and implications for restoration. *New Phytologist*,
722 247(3), 1081–1097. <https://doi.org/10.1111/nph.70247>

723 Cole, R. J., Werden, L. K., Arroyo, F. C., Quirós, K. M., Cedeño, G. Q., & Crowther, T. W.
724 (2024). Forest restoration in practice across Latin America. *Biological Conservation*,
725 294, 110608. <https://doi.org/10.1016/j.biocon.2024.110608>

726 Coverdale, T. C., & Davies, A. B. (2023). Unravelling the relationship between plant
727 diversity and vegetation structural complexity: A review and theoretical framework.
728 *Journal of Ecology*, 111(7), 1378–1395. <https://doi.org/10.1111/1365-2745.14068>

729 Crouzeilles, R., Beyer, H. L., Monteiro, L. M., Feltran-Barbieri, R., Pessôa, A. C. M., Barros,
730 F. S. M., Lindenmayer, D. B., Lino, E. D. S. M., Grelle, C. E. V., Chazdon, R. L.,
731 Matsumoto, M., Rosa, M., Latawiec, A. E., & Strassburg, B. B. N. (2020). Achieving
732 cost-effective landscape-scale forest restoration through targeted natural regeneration.
733 *Conservation Letters*, 13(3), 1–9. <https://doi.org/10.1111/conl.12709>

734 Depauw, L., De Lombaerde, E., Dhiedt, E., Blondeel, H., Abdala-Roberts, L., Auge, H.,
735 Barsoum, N., Bauhus, J., Chu, C., Damtew, A., Eisenhauer, N., Fagundes, M. V.,
736 Ganade, G., Gendreau-Berthiaume, B., Godbold, D., Gravel, D., Guillemot, J., Hajek,
737 P., Hector, A., ... Baeten, L. (2024). Enhancing Tree Performance Through Species
738 Mixing: Review of a Quarter-Century of TreeDivNet Experiments Reveals Research
739 Gaps and Practical Insights. *Current Forestry Reports*, 10(1), 1–20.
740 <https://doi.org/10.1007/s40725-023-00208-y>

741 Díaz, S., Lavorel, S., Chapin, F. S., Tecco, P. A., Gurvich, D. E., & Grigulis, K. (2007).
742 Functional Diversity—At the Crossroads between Ecosystem Functioning and
743 Environmental Filters. In J. G. Canadell, D. E. Pataki, & L. F. Pitelka (Eds.),
744 *Terrestrial Ecosystems in a Changing World* (pp. 81–91). Springer Berlin Heidelberg.
745 https://doi.org/10.1007/978-3-540-32730-1_7

746 Elmqvist, T., Folke, C., Nyström, M., Peterson, G., Bengtsson, J., Walker, B., & Norberg, J.
747 (2003). Response diversity, ecosystem change, and resilience. *Frontiers in Ecology*
748 *and the Environment*, *1*(9), 488–494. [https://doi.org/10.1890/1540-](https://doi.org/10.1890/1540-9295(2003)001%5B0488:RDECAR%5D2.0.CO;2)
749 [9295\(2003\)001%5B0488:RDECAR%5D2.0.CO;2](https://doi.org/10.1890/1540-9295(2003)001%5B0488:RDECAR%5D2.0.CO;2)

750 Fremout, T., Gutiérrez-Miranda, C. E., Briers, S., Marcelo-Peña, J. L., Cueva-Ortiz, E.,
751 Linares-Palomino, R., La Torre-Cuadros, M. de los Á., Chang-Ruíz, J. C., Villegas-
752 Gómez, T. L., Acosta-Flota, A. H., Plouvier, D., Atkinson, R., Charcape-Ravelo, M.,
753 Aguirre-Mendoza, Z., Muys, B., & Thomas, E. (2021). The value of local ecological
754 knowledge to guide tree species selection in tropical dry forest restoration.
755 *Restoration Ecology*, *29*(4), e13347. <https://doi.org/10.1111/rec.13347>

756 Gornish, E. S., Campbell, C., Svejcar, L., Munson, S. M., Vaughn, K., Spaeth, M. K.,
757 Yelenik, S. G., Wolf, A., & Mitchell, R. (2023). Functional traits are used in
758 restoration practice: A response to Merchant et al. (2022). *Restoration Ecology*, *31*(7),
759 e13880. <https://doi.org/10.1111/rec.13880>

760 Griscom, B. W., Adams, J., Ellis, P. W., Houghton, R. A., Lomax, G., Miteva, D. A.,
761 Schlesinger, W. H., Shoch, D., Siikamäki, J. V., Smith, P., Woodbury, P., Zganjar, C.,
762 Blackman, A., Campari, J., Conant, R. T., Delgado, C., Elias, P., Gopalakrishna, T.,
763 Hamsik, M. R., ... Fargione, J. (2017). Natural climate solutions. *Proceedings of the*
764 *National Academy of Sciences*, *114*(44), 11645–11650.
765 <https://doi.org/10.1073/pnas.1710465114>

766 Griscom, B. W., Lomax, G., Kroeger, T., Fargione, J. E., Adams, J., Almond, L., Bossio, D.,
767 Cook-Patton, S. C., Ellis, P. W., Kennedy, C. M., & Kiesecker, J. (2019). We need
768 both natural and energy solutions to stabilize our climate. *Global Change Biology*,
769 25(6), 1889–1890. <https://doi.org/10.1111/gcb.14612>

770 Hector, A., Hautier, Y., Saner, P., Wacker, L., Bagchi, R., Joshi, J., Scherer-Lorenzen, M.,
771 Spehn, E. M., Bazeley-White, E., Weilenmann, M., Caldeira, M. C., Dimitrakopoulos,
772 P. G., Finn, J. A., Huss-Danell, K., Jumpponen, A., Mulder, C. P. H., Palmborg, C.,
773 Pereira, J. S., Siamantziouras, A. S. D., ... Loreau, M. (2010). General stabilizing
774 effects of plant diversity on grassland productivity through population asynchrony and
775 overyielding. *Ecology*, 91(8), 2213–2220. <https://doi.org/10.1890/09-1162.1>

776 Holdridge, L. R., Grenke, W. C., Hatheway, W. H., Liang, T., & Tosi, J. A. (1971). *Forest*
777 *environments in tropical life zones*. Pergamon Press.

778 Holl, K. D. (2017). Restoring tropical forests from the bottom up. *Science*, 355(6324), 455–
779 456. <https://doi.org/10.1126/science.aam5432>

780 Holl, K. D., Luong, J. C., & Brancalion, P. H. S. (2022). Overcoming biotic homogenization
781 in ecological restoration. *Trends in Ecology & Evolution*, S0169534722001136.
782 <https://doi.org/10.1016/j.tree.2022.05.002>

783 Holl, K. D., Stout, V. M., Reid, J. L., & Zahawi, R. A. (2013). Testing heterogeneity–
784 diversity relationships in tropical forest restoration. *Oecologia*, 173(2), 569–578.
785 <https://doi.org/10.1007/s00442-013-2632-9>

786 Holl, K. D., Zahawi, R. A., Cole, R. J., Ostertag, R., & Cordell, S. (2011). Planting Seedlings
787 in Tree Islands Versus Plantations as a Large-Scale Tropical Forest Restoration
788 Strategy. *Restoration Ecology*, 19(4), 470–479. [https://doi.org/10.1111/j.1526-](https://doi.org/10.1111/j.1526-100X.2010.00674.x)
789 [100X.2010.00674.x](https://doi.org/10.1111/j.1526-100X.2010.00674.x)

790 Huang, Y., Chen, Y., Castro-Izaguirre, N., Baruffol, M., Brezzi, M., Lang, A., Li, Y.,
791 Härdtle, W., Von Oheimb, G., Yang, X., Liu, X., Pei, K., Both, S., Yang, B.,
792 Eichenberg, D., Assmann, T., Bauhus, J., Behrens, T., Buscot, F., ... Schmid, B.
793 (2018). Impacts of species richness on productivity in a large-scale subtropical forest
794 experiment. *Science*, 362(6410), 80–83. <https://doi.org/10.1126/science.aat6405>

795 Isbell, F., Craven, D., Connolly, J., Loreau, M., Schmid, B., Beierkuhnlein, C., Bezemer, T.
796 M., Bonin, C., Bruelheide, H., De Luca, E., Ebeling, A., Griffin, J. N., Guo, Q.,
797 Hautier, Y., Hector, A., Jentsch, A., Kreyling, J., Lanta, V., Manning, P., ...
798 Eisenhauer, N. (2015). Biodiversity increases the resistance of ecosystem productivity
799 to climate extremes. *Nature*, 526(7574), 574–577.
800 <https://doi.org/10.1038/nature15374>

801 Kattge, J., Bönisch, G., Díaz, S., Lavorel, S., Prentice, I. C., Leadley, P., Tautenhahn, S.,
802 Werner, G. D. A., Aakala, T., Abedi, M., Acosta, A. T. R., Adamidis, G. C.,
803 Adamson, K., Aiba, M., Albert, C. H., Alcántara, J. M., Alcázar C, C., Aleixo, I., Ali,
804 H., ... Wirth, C. (2020). TRY plant trait database – enhanced coverage and open
805 access. *Global Change Biology*, 26(1), 119–188. <https://doi.org/10.1111/gcb.14904>

806 Laughlin, D. C. (2014). Applying trait-based models to achieve functional targets for theory-
807 driven ecological restoration. *Ecology Letters*, 17(7), 771–784.
808 <https://doi.org/10.1111/ele.12288>

809 Lewis, S. L., Edwards, D. P., & Galbraith, D. (2015). Increasing human dominance of
810 tropical forests. *Science*, 349(6250), 827–832.
811 <https://doi.org/10.1126/science.aaa9932>

812 Liang, J., Crowther, T. W., Picard, N., Wiser, S., Zhou, M., Alberti, G., Schulze, E.-D.,
813 McGuire, A. D., Bozzato, F., Pretzsch, H., de-Miguel, S., Paquette, A., Hérault, B.,
814 Scherer-Lorenzen, M., Barrett, C. B., Glick, H. B., Hengeveld, G. M., Nabuurs, G.-J.,

815 Pfautsch, S., ... Reich, P. B. (2016). Positive biodiversity-productivity relationship
816 predominant in global forests. *Science*, 354(6309), aaf8957.
817 <https://doi.org/10.1126/science.aaf8957>

818 Liu, X., Schuldt, A., Cavender-Bares, J., Paquette, A., Schmid, B., & Ma, K. (2026).
819 Ecological insights from three decades of forest biodiversity experiments. *Nature*
820 *Reviews Biodiversity*, 2(1), 9–23. <https://doi.org/10.1038/s44358-025-00112-2>

821 Loreau, M., & De Mazancourt, C. (2013). Biodiversity and ecosystem stability: A synthesis
822 of underlying mechanisms. *Ecology Letters*, 16(s1), 106–115.
823 <https://doi.org/10.1111/ele.12073>

824 Maitner, B. S., Boyle, B., Casler, N., Condit, R., Donoghue, J., Durán, S. M., Guaderrama,
825 D., Hinchliff, C. E., Jørgensen, P. M., Kraft, N. J. B., McGill, B., Merow, C.,
826 Morueta-Holme, N., Peet, R. K., Sandel, B., Schildhauer, M., Smith, S. A., Svenning,
827 J.-C., Thiers, B., ... Enquist, B. J. (2018). The bien r package: A tool to access the
828 Botanical Information and Ecology Network (BIEN) database. *Methods in Ecology*
829 *and Evolution*, 9(2), 373–379. <https://doi.org/10.1111/2041-210X.12861>

830 Malhi, Y., Gardner, T. A., Goldsmith, G. R., Silman, M. R., & Zelazowski, P. (2014).
831 Tropical Forests in the Anthropocene. *Annual Review of Environment and Resources*,
832 39(1), 125–159. <https://doi.org/10.1146/annurev-environ-030713-155141>

833 Maynard, D. S., Bialic-Murphy, L., Zohner, C. M., Averill, C., Van Den Hoogen, J., Ma, H.,
834 Mo, L., Smith, G. R., Acosta, A. T. R., Aubin, I., Berenguer, E., Boonman, C. C. F.,
835 Catford, J. A., Cerabolini, B. E. L., Dias, A. S., González-Melo, A., Hietz, P., Lusk,
836 C. H., Mori, A. S., ... Crowther, T. W. (2022). Global relationships in tree functional
837 traits. *Nature Communications*, 13(1), 3185. [https://doi.org/10.1038/s41467-022-](https://doi.org/10.1038/s41467-022-30888-2)
838 [30888-2](https://doi.org/10.1038/s41467-022-30888-2)

839 Menalled, F. D., Kelty, M. J., & Ewel, J. J. (1998). Canopy development in tropical tree
840 plantations: A comparison of species mixtures and monocultures. *Forest Ecology and*
841 *Management*, 104(1–3), 249–263. [https://doi.org/10.1016/S0378-1127\(97\)00255-7](https://doi.org/10.1016/S0378-1127(97)00255-7)

842 Ostertag, R., Warman, L., Cordell, S., & Vitousek, P. M. (2015). Using plant functional traits
843 to restore Hawaiian rainforest. *Journal of Applied Ecology*, 52(4), 805–809.
844 <https://doi.org/10.1111/1365-2664.12413>

845 Paterno, G. B., Brambach, F., Guerrero-Ramírez, N., Zemp, D. C., Cantillo, A. F.,
846 Camarretta, N., Moura, C. C. M., Gailing, O., Ballauff, J., Polle, A., Schlund, M.,
847 Erasmi, S., Iddris, N. A., Khokthong, W., Sundawati, L., Irawan, B., Hölscher, D., &
848 Kreft, H. (2024). Diverse and larger tree islands promote native tree diversity in oil
849 palm landscapes. *Science*, 386(6723), 795–802.
850 <https://doi.org/10.1126/science.ad01629>

851 Perles-Garcia, M. D., Kunz, M., Fichtner, A., Härdtle, W., & Von Oheimb, G. (2021). Tree
852 species richness promotes an early increase of stand structural complexity in young
853 subtropical plantations. *Journal of Applied Ecology*, 58(10), 2305–2314.
854 <https://doi.org/10.1111/1365-2664.13973>

855 Petchey, O. L., & Gaston, K. J. (2002). Functional diversity (FD), species richness and
856 community composition. *Ecology Letters*, 5(3), 402–411.
857 <https://doi.org/10.1046/j.1461-0248.2002.00339.x>

858 Pillay, R., Venter, M., Aragon-Osejo, J., González-del-Pliego, P., Hansen, A. J., Watson, J.
859 E., & Venter, O. (2022). Tropical forests are home to over half of the world's
860 vertebrate species. *Frontiers in Ecology and the Environment*, 20(1), 10–15.
861 <https://doi.org/10.1002/fee.2420>

862 Pinnschmidt, A., Yousefpour, R., Nölte, A., Murillo, O., & Hanewinkel, M. (2023).
863 Economic potential and management of tropical mixed-species plantations in Central
864 America. *New Forests*, 54(3), 565–586. <https://doi.org/10.1007/s11056-022-09937-7>

865 R Development Core Team. (2025). *R: A language and environment for statistical*
866 *computing. Version 4.5.0*. <https://www.r-project.org/>

867 Rayome, D., DiManno, N., Ostertag, R., Cordell, S., Fung, B., Vizzone, A., Pante, P., & Tate,
868 R. (2019). *Restoring Ecosystem Services Tool (REST): A program for selecting*
869 *species for restoration projects using a functional-trait approach* (PSW-GTR-262; p.
870 PSW-GTR-262). U.S. Department of Agriculture, Forest Service, Pacific Southwest
871 Research Station. <https://doi.org/10.2737/PSW-GTR-262>

872 Réjou-Méchain, M., Tanguy, A., Piponiot, C., Chave, J., & Hérault, B. (2017). BIOMASS: An
873 R package for estimating above-ground biomass and its uncertainty in tropical forests.
874 *Methods in Ecology and Evolution*, 8(9), 1163–1167. [https://doi.org/10.1111/2041-](https://doi.org/10.1111/2041-210X.12753)
875 [210X.12753](https://doi.org/10.1111/2041-210X.12753)

876 Schindler, D. E., Armstrong, J. B., & Reed, T. E. (2015). The portfolio concept in ecology
877 and evolution. *Frontiers in Ecology and the Environment*, 13(5), 257–263.
878 <https://doi.org/10.1890/140275>

879 Schnabel, F., Guillemot, J., Barry, K. E., Brunn, M., Cesarz, S., Eisenhauer, N., Gebauer, T.,
880 Guerrero-Ramirez, N. R., Handa, I. T., Madsen, C., Mancilla, Lady, Monteza, J.,
881 Moore, T., Oelmann, Y., Scherer-Lorenzen, M., Schwendenmann, L., Wagner, A.,
882 Wirth, C., & Potvin, C. (2025). Tree Diversity Increases Carbon Stocks and Fluxes
883 Above-But Not Belowground in a Tropical Forest Experiment. *Global Change*
884 *Biology*, 31(2), e70089. <https://doi.org/10.1111/gcb.70089>

885 Schnabel, F., Schwarz, J. A., Dănescu, A., Fichtner, A., Nock, C. A., Bauhus, J., & Potvin, C.
886 (2019). Drivers of productivity and its temporal stability in a tropical tree diversity

887 experiment. *Global Change Biology*, 25(12), 4257–4272.
888 <https://doi.org/10.1111/gcb.14792>

889 Seddon, N., Smith, A., Smith, P., Key, I., Chausson, A., Girardin, C., House, J., Srivastava,
890 S., & Turner, B. (2021). Getting the message right on nature-based solutions to
891 climate change. *Global Change Biology*, 27(8), 1518–1546.
892 <https://doi.org/10.1111/gcb.15513>

893 Specker, F., Paz, A., Crowther, T. W., & Maynard, D. S. (2024). Tremendous: An R
894 package for integrating taxonomic information across backbones. *PeerJ*, 12, e16896.
895 <https://doi.org/10.7717/peerj.16896>

896 Stanturf, J. A. (2021). Landscape degradation and restoration. In *Soils and Landscape*
897 *Restoration* (pp. 125–159). Elsevier. [https://doi.org/10.1016/B978-0-12-813193-](https://doi.org/10.1016/B978-0-12-813193-0.00005-9)
898 [0.00005-9](https://doi.org/10.1016/B978-0-12-813193-0.00005-9)

899 Tilman, D. (1999). THE ECOLOGICAL CONSEQUENCES OF CHANGES IN
900 BIODIVERSITY: A SEARCH FOR GENERAL PRINCIPLES. *Ecology*, 80(5),
901 1455–1474. [https://doi.org/10.1890/0012-](https://doi.org/10.1890/0012-9658(1999)080%5B1455:TECOCI%5D2.0.CO;2)
902 [9658\(1999\)080%5B1455:TECOCI%5D2.0.CO;2](https://doi.org/10.1890/0012-9658(1999)080%5B1455:TECOCI%5D2.0.CO;2)

903 Van De Peer, T., Verheyen, K., Baeten, L., Ponette, Q., & Muys, B. (2016). Biodiversity as
904 insurance for sapling survival in experimental tree plantations. *Journal of Applied*
905 *Ecology*, 53(6), 1777–1786. <https://doi.org/10.1111/1365-2664.12721>

906 Verbiest, W. W. M., Hicter, P., Beeckman, H., Wallenus, D., Ilondea, B. A., Bastin, J.-F.,
907 Bauters, M., Chave, J., De Blaere, R., de Hauleville, T., De Mil, T., de Ridder, M., De
908 Troyer, C., Ewango, C. E. N., Fayolle, A., Gorel, A., Fischer, F. J., Kaçamak, B.,
909 Kimbuluma, C., ... Hubau, W. (2026). The Tervuren xylarium Wood Density
910 Database (TWDD). *Scientific Data*. <https://doi.org/10.1038/s41597-026-06563-2>

911 Verheyen, K., Vanhellefont, M., Auge, H., Baeten, L., Baraloto, C., Barsoum, N., Bilodeau-
912 Gauthier, S., Bruelheide, H., Castagneyrol, B., Godbold, D., Haase, J., Hector, A.,
913 Jactel, H., Koricheva, J., Loreau, M., Mereu, S., Messier, C., Muys, B., Nolet, P., ...
914 Scherer-Lorenzen, M. (2016). Contributions of a global network of tree diversity
915 experiments to sustainable forest plantations. *Ambio*, 45(1), 29–41.
916 <https://doi.org/10.1007/s13280-015-0685-1>

917 Veryard, R., Wu, J., O'Brien, M. J., Anthony, R., Both, S., Burslem, D. F. R. P., Chen, B.,
918 Fernandez-Miranda Cagigal, E., Godfray, H. C. J., Godoong, E., Liang, S., Saner, P.,
919 Schmid, B., Sau Wai, Y., Xie, J., Reynolds, G., & Hector, A. (2023). Positive effects
920 of tree diversity on tropical forest restoration in a field-scale experiment. *Science*
921 *Advances*, 9(37), eadf0938. <https://doi.org/10.1126/sciadv.adf0938>

922 Vieilledent, G., Fischer, F. J., Chave, J., Guibal, D., Langbour, P., & Gérard, J. (2017). *The*
923 *Cirad wood density database* [Dataset]. Zenodo.
924 <https://doi.org/10.5281/zenodo.1095454>

925 Warner, E., Cook-Patton, S. C., Lewis, O. T., Brown, N., Koricheva, J., Eisenhauer, N.,
926 Ferlian, O., Gravel, D., Hall, J. S., Jactel, H., Mayoral, C., Meredieu, C., Messier, C.,
927 Paquette, A., Parker, W. C., Potvin, C., Reich, P. B., & Hector, A. (2023). Young
928 mixed planted forests store more carbon than monocultures—A meta-analysis.
929 *Frontiers in Forests and Global Change*, 6.
930 <https://www.frontiersin.org/articles/10.3389/ffgc.2023.1226514>

931 Werden, L. K., Alvarado J, P., Zarges, S., Calderón M, E., Schilling, E. M., Gutiérrez L, M.,
932 & Powers, J. S. (2018). Using soil amendments and plant functional traits to select
933 native tropical dry forest species for the restoration of degraded Vertisols. *Journal of*
934 *Applied Ecology*, 55(2), 1019–1028. <https://doi.org/10.1111/1365-2664.12998>

935 Yachi, S., & Loreau, M. (1999). Biodiversity and ecosystem productivity in a fluctuating
936 environment: The insurance hypothesis. *Proceedings of the National Academy of*
937 *Sciences*, 96(4), 1463–1468. <https://doi.org/10.1073/pnas.96.4.1463>

938 Zhang, Y., Chen, H. Y. H., & Reich, P. B. (2012). Forest productivity increases with
939 evenness, species richness and trait variation: A global meta-analysis. *Journal of*
940 *Ecology*, 100(3), 742–749. <https://doi.org/10.1111/j.1365-2745.2011.01944.x>

941

Supplementary material for:

Species diversity reduces risk in tropical forest restoration: a portfolio effect across heterogeneous sites

Rachele Quaglino^{1,φ,*}, Rebecca J. Cole^{1,2,φ}, Gerald Quirós Cedeno^{1,2}, David Rodríguez³, Jeff Tingle⁴, Daniel S. Maynard⁵, Anton Weissenhofer⁶, Thomas Crowther^{7,8}, Leland K. Werden^{1,φ,*}

¹Department of Environmental Systems Science, ETH Zürich, Zürich, Switzerland

²Tropical Landscape and Climate Program, Agua Buena, Puntarenas Province, Costa Rica

³Finca Cántaros Environmental Association, San Vito, Puntarenas Province, Costa Rica

⁴Finca Aguas Buenas, Filadelfia de Buenos Aires, Puntarenas, Costa Rica

⁵Department of Genetics, Evolution and Environment, University College London, London, United Kingdom

⁶University of Vienna, Department of Botany and Biodiversity Research, Vienna, Austria

⁷BRANCH Institute, Zug, Switzerland

⁸King Abdullah University of Science and Technology (KAUST), Thuwal, Saudi Arabia

Figures

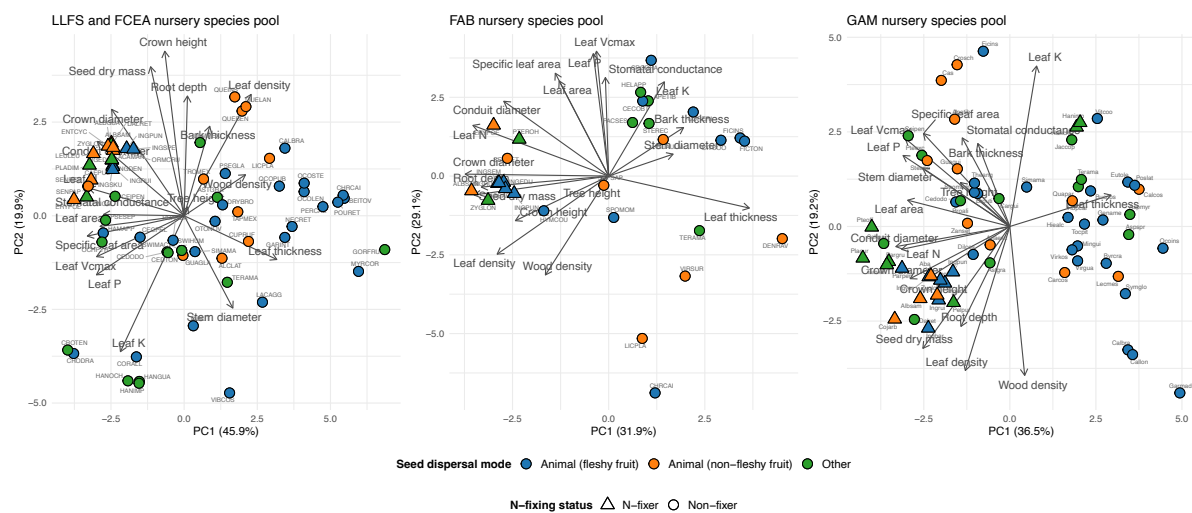


Figure S1. Principal components analysis of functional trait space for the nursery species pool at each site. Species codes are the first three letters of the genus and the first three letters of the specific epithet (e.g., INGEDU = *Inga edulis*; see Table S3 for full names). Each point represents a candidate species, colored by seed dispersal mode and shaped by nitrogen-fixing status. Loading arrows show the contribution of 18 imputed functional traits (Table S2) to the first two principal components. LLFS and FCEA, FAB, and GAM. Species were selected at each richness level to maximize trait space occupancy (Table S3)

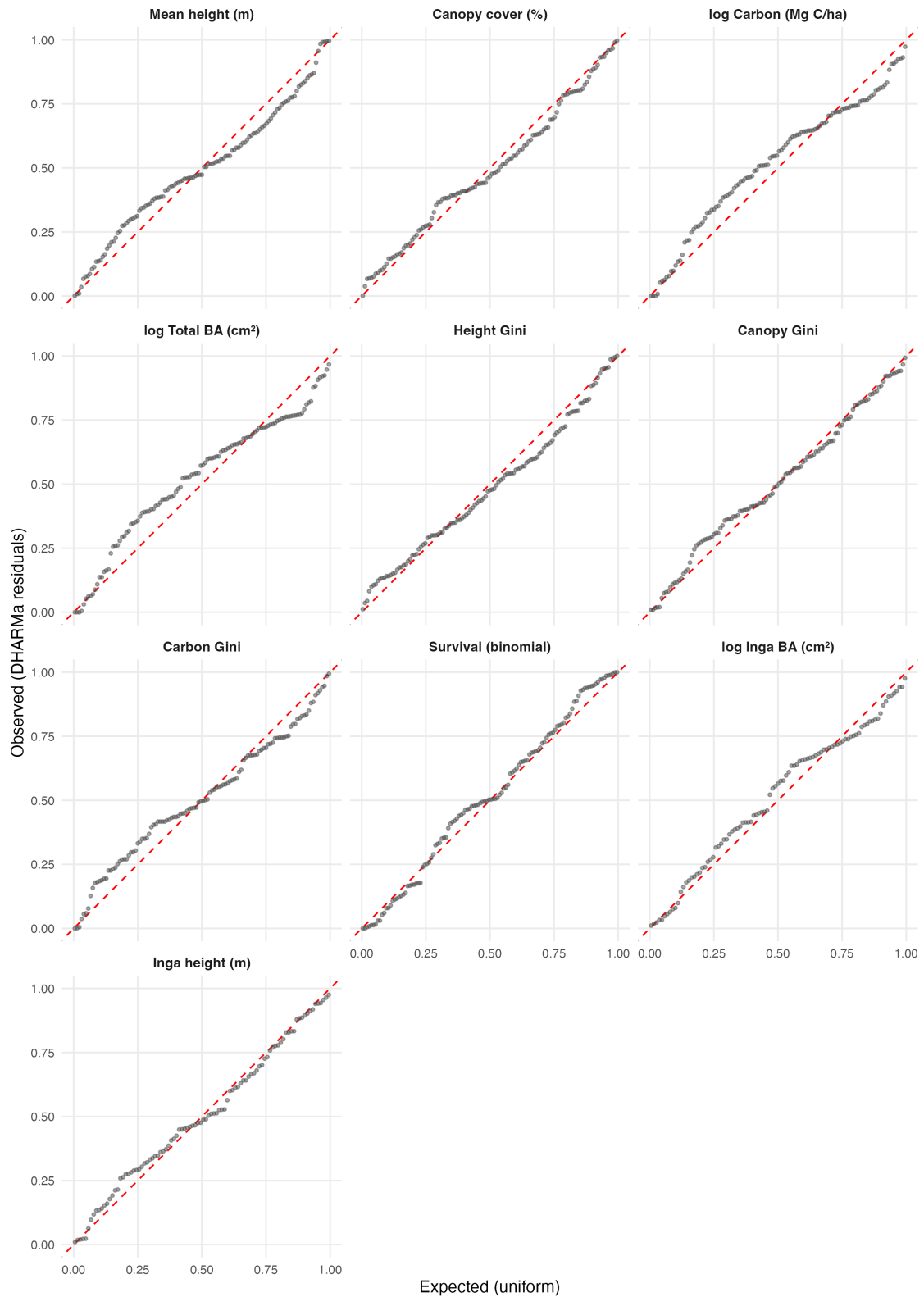


Figure S2. Quantile-quantile plots of DHARMA simulated residuals for all mixed-effects models. Each panel shows one response variable; the dashed red line indicates the expected uniform distribution. Carbon, total basal area, and *Inga* basal area were log-transformed; survival was modeled as a binomial GLMM (glmmTMB).

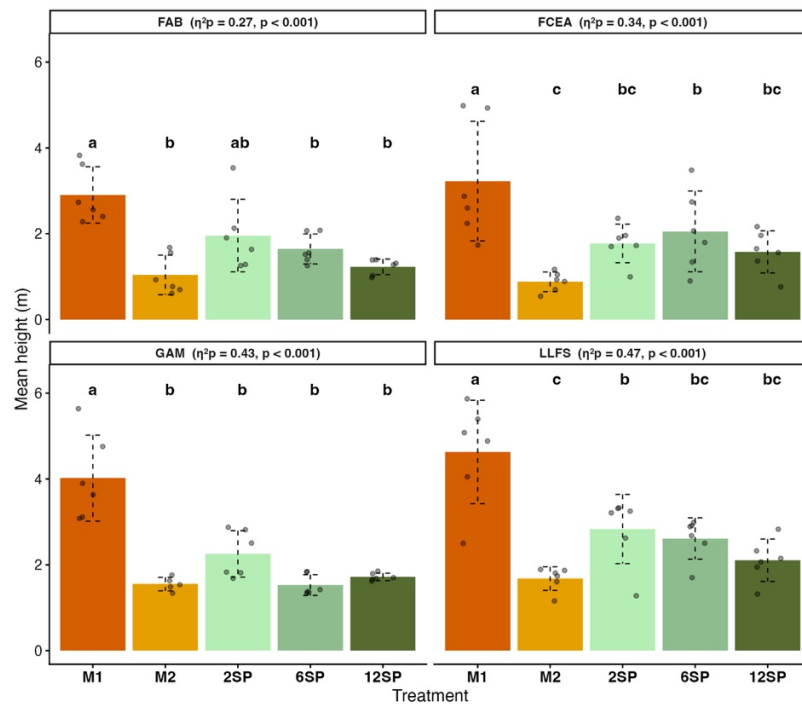


Figure S3. Mean tree height (m) by treatment at each site after three years. Bars show treatment means; error bars show standard deviations; points are individual plots (N = 6 per treatment per site). Letters denote significant pairwise differences (Tukey HSD, $p < 0.05$). Partial eta-squared (η^2p) and p-values for the treatment effect are shown for each site.

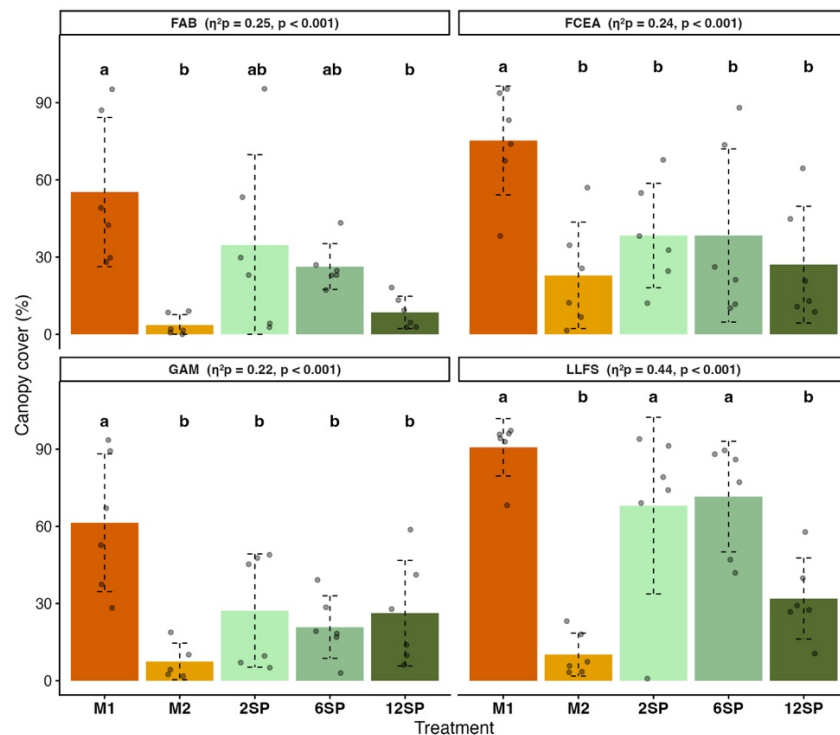


Figure S4. Canopy cover (%) by treatment at each site after three years. Statistics reported as in Figure S3.

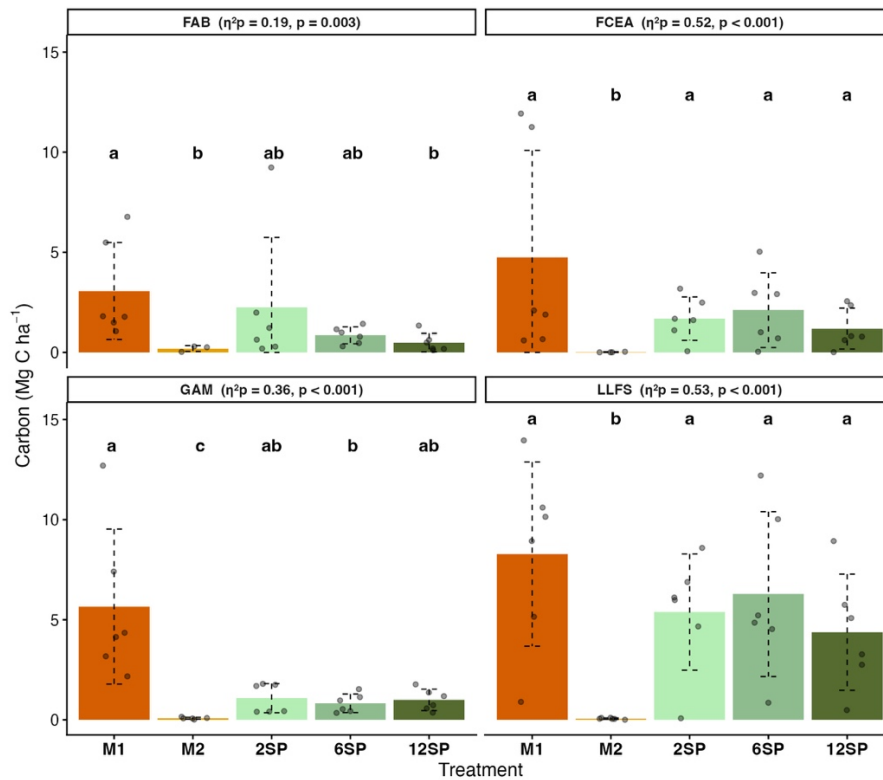


Figure S5. Carbon stocks (Mg C ha⁻¹) by treatment at each site after three years. Statistics reported as in Figure S3.

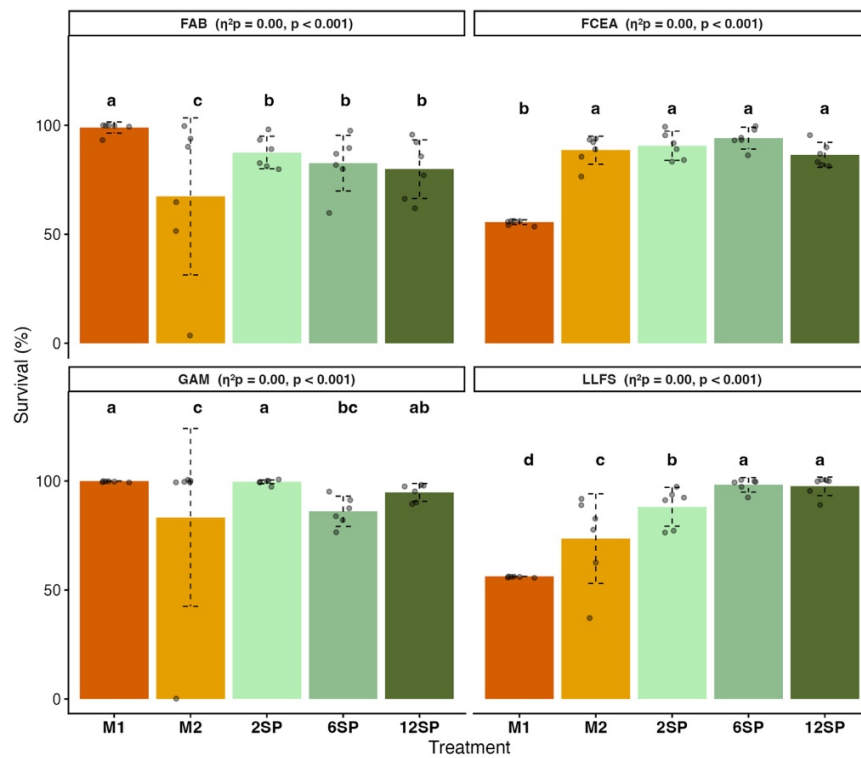


Figure S6. Survival (%) by treatment at each site after three years. Statistics reported as in Figure S3. Survival was modeled as a binomial GLMM; pairwise letters are Sidak-adjusted, not Tukey.

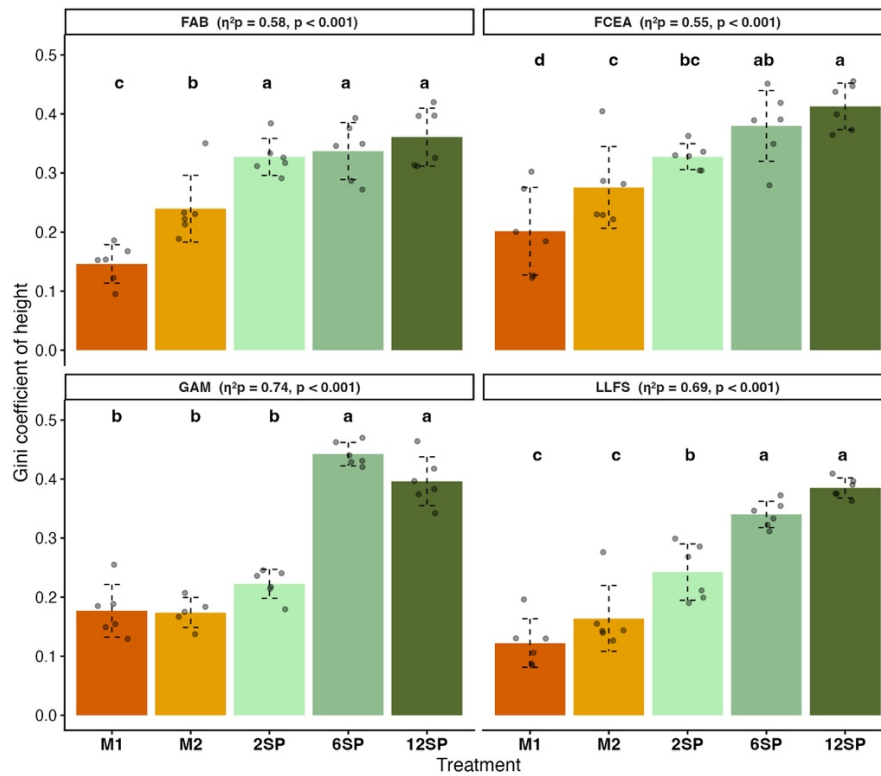


Figure S7. Within-plot height heterogeneity (Gini coefficient) by treatment at each site after three years. Statistics reported as in Figure S3.

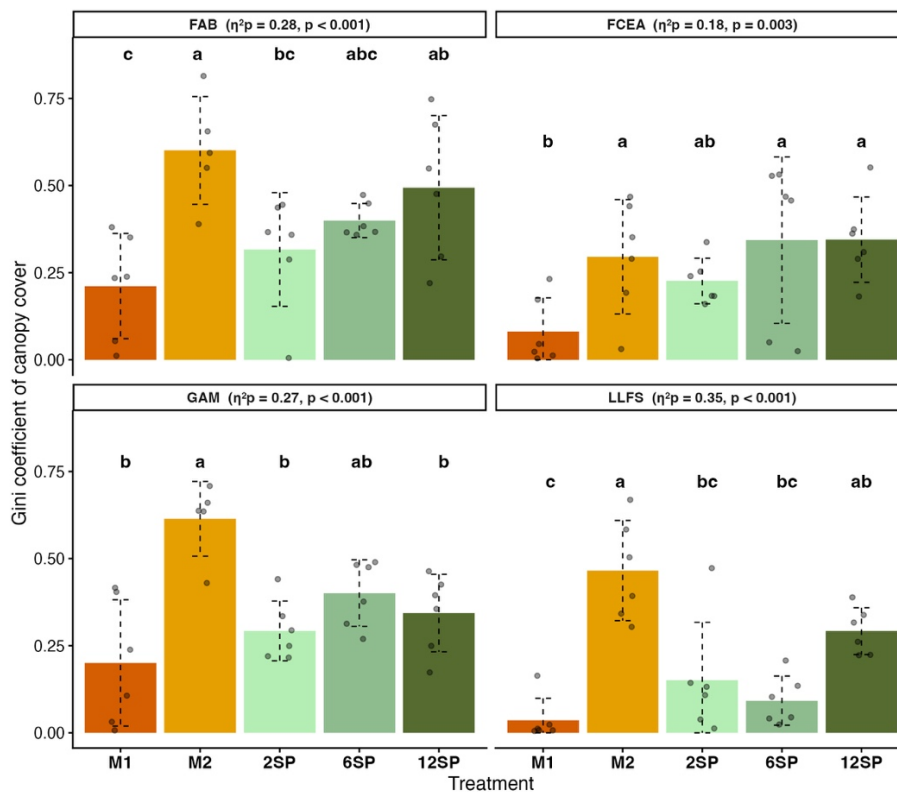


Figure S8. Within-plot canopy cover heterogeneity (Gini coefficient) by treatment at each site after three years. Statistics reported as in Figure S3.

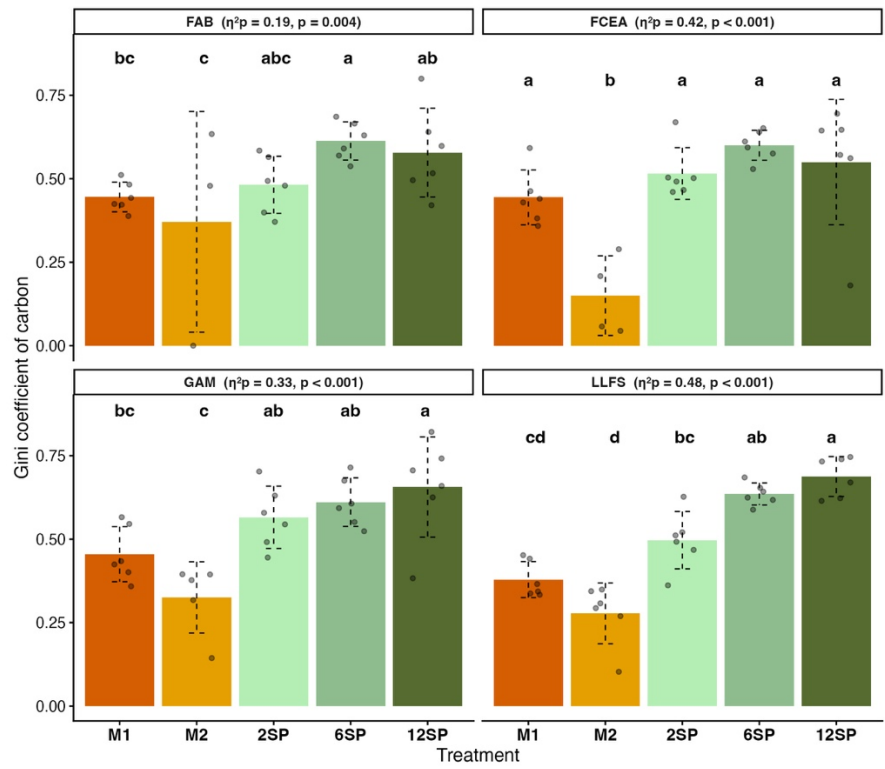


Figure S9. Within-plot carbon heterogeneity (Gini coefficient) by treatment at each site after three years. Statistics reported as in Figure S3.

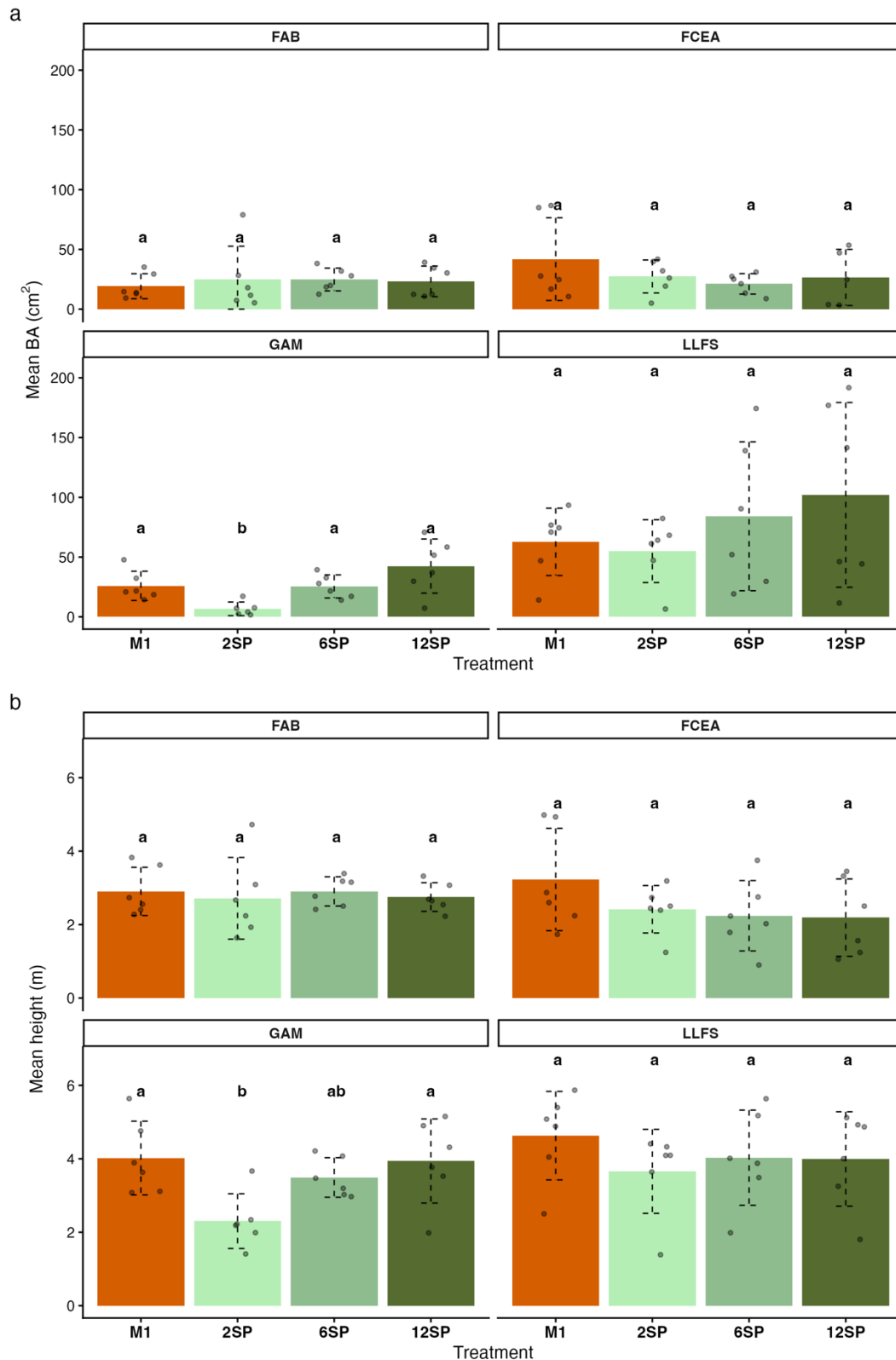


Figure S10. Individual-level performance of *Inga edulis* across treatments at each site. (a) Mean individual basal area (cm²) and (b) mean individual height (m) in M1 (monoculture) versus mixed-species treatments (2SP, 6SP, 12SP). M2 is excluded because it does not contain *Inga*.

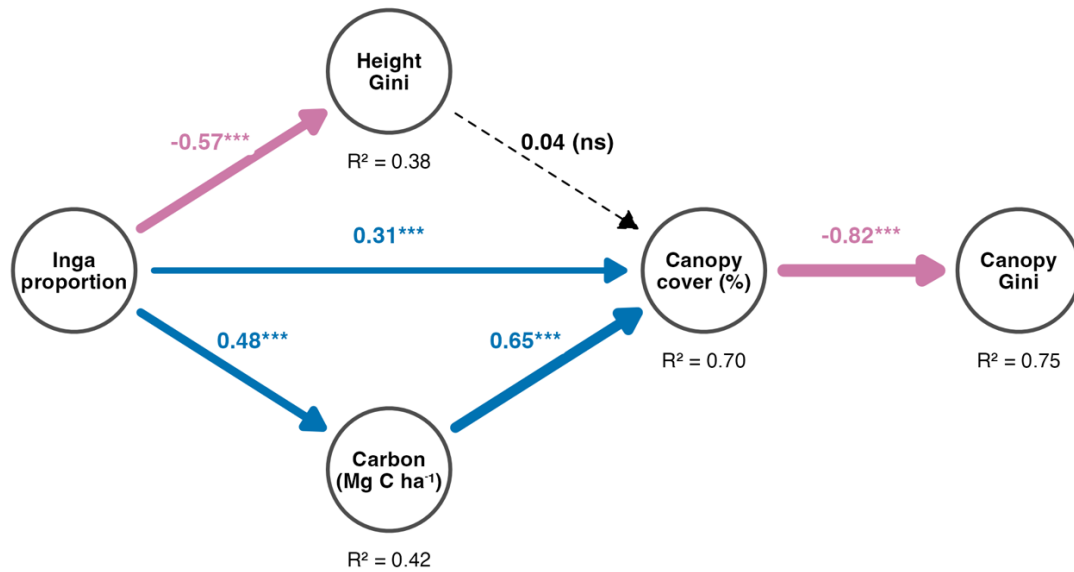


Figure S11. Piecewise structural equation model of Figure 5 recoded with *Inga edulis* proportion in place of log-transformed species richness (all five treatments included). Because *I. edulis* proportion is collinear with planted richness by design, this is not an independent test but confirms that the structural pathways are not an artifact of the richness coding. Arrow colors and widths as in Figure 5; R^2 values are conditional (including the site-level random effect).

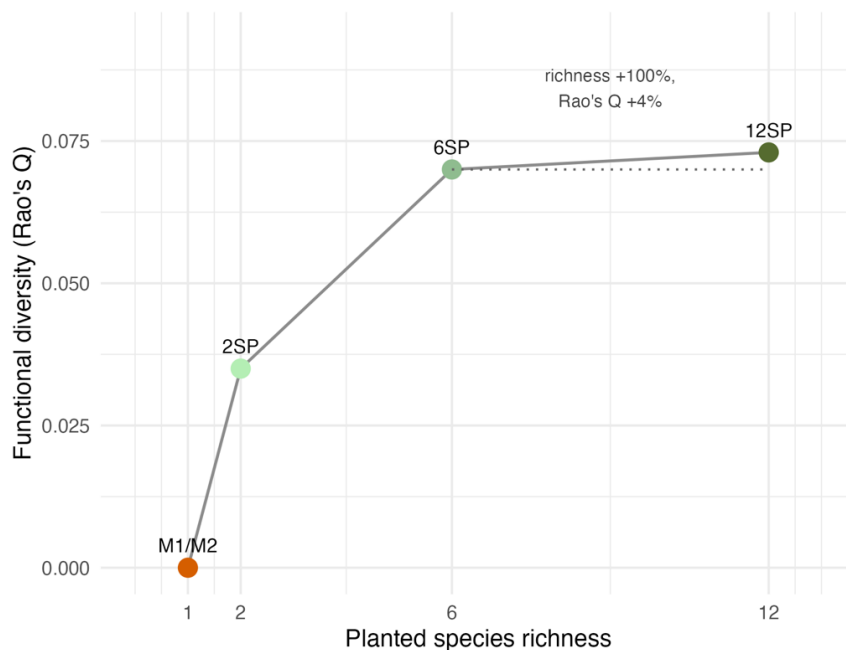


Figure S12. Functional diversity saturates along the planted-richness gradient. Functional diversity (Rao's Q) per treatment, averaged across the four sites, rises from monocultures (0) through two- and six-species mixes (~0.035, 0.070, respectively) then levels off. Doubling richness from six to twelve species increases Rao's Q by ~4% on average across sites (to 0.073), so the additional species appear largely functionally redundant. (The dispersion scale-robustness and survival-variability results are presented in Tables S5 and S7)

Tables

Table S1. Details on the restoration sites in southwestern Costa Rica.

Site	Site Code	Coordinates	Elevation	Mean Annual Rainfall	Mean Annual Temperature	Land Use History
Finca Aguas Buenas	FAB	N: 9°1'16", W:83°29'22"	930 m	4100 mm	22 °C	Cattle Grazing
Finca Cantaros Environmental Association	FCEA	N: 8°47'58", W:82°57'51"	1100 m	4000 mm	21 °C	Cattle Grazing
Loma Linda Field Station	LLFS	N: 8°44'31", W:82°55'33"	1160 m	3800 mm	21°C	Cattle Grazing, Mixed Agriculture
La Gamba Tropical Station	GAM	N: 8°45'17.8 W: 83°08'41.2	450 m	6,140 mm	28 °C	Cattle Grazing

Table S2. List of functional traits and units used to design tree species mixes for the treatments

Functional trait	Units
Bark thickness	mm
Crown diameter, maximum	m
Crown height, maximum	m
Leaf area	cm ²
Leaf density	g cm ⁻³
Leaf K per mass	mg g ⁻¹
Leaf N per mass	mg g ⁻¹
Leaf P per mass	mg g ⁻¹
Leaf thickness	mm
Leaf V _{cmax}	μmol g ⁻¹ s ⁻¹
Root depth, maximum	m
Seed dry mass	mg
Specific leaf area	mm ² mg ⁻¹
Stem conduit diameter	μm
Stem diameter	m
Stomatal conductance	mmol m ⁻² s ⁻¹
Tree height, maximum	m
Wood density	g _{dry} cm _{wet} ⁻³

Table S3. Species used in the experiment and their allocation across sites and treatments (species denoted with * were planted in 6-species mix only at LLFS)

Species	Common Name	Site	Treatment Codes
<i>Aspidosperma myristicifolium</i>	Guatambu	GAM	6SP, 12SP
<i>Astronium graveolens</i>	Ron Ron	GAM	12SP
<i>Calophyllum brasiliense</i>	Santa Maria	LLFS	M2, 2SP, 6SP, 12SP
<i>Cedrela tonduzii</i>	Cedro dulce	FCEA	12SP
<i>Chrysophyllum cainito</i>	Caimito	FAB	12SP
<i>Citharexylum cooperi</i>	Dama	GAM	M2, 2SP, 6SP, 12SP
<i>Cojoba arborea</i>	Lorito	GAM	12SP
<i>Cordia alliodora</i>	Laurel	FCEA, LLFS	12SP
<i>Croton draco</i>	Targua	FCEA, LLFS	6SP, 12SP
<i>Croton schiedeana</i>	Colpachi	GAM	6SP, 12SP
<i>Cupania rufescens</i>	Guavillo	FCEA	12SP
<i>Dendropanax ravenii</i>	Fosforillo	FAB	12SP
<i>Erythrina poeppigiana</i>	Poro	FAB, FCEA, LLFS	12SP
<i>Ficus insipida</i>	Higueron	FAB	M2, 2SP, 6SP, 12SP
<i>Ficus maxima</i>	Higueron	GAM	12SP
<i>Garcinia madruno</i>	Madrono	GAM	6SP, 12SP
<i>Handroanthus impetiginosus</i>	Roble de sabana	GAM	12SP
<i>Handroanthus ochraceus</i>	Corteza amarilla	LLFS	12SP
<i>Heliocarpus appendiculatus</i>	Burio	FAB, FCEA	6SP, 12SP
<i>Inga edulis</i>	Guaba	FAB, FCEA, LLFS, GAM	M1, 2SP, 6SP, 12SP
<i>Lacistema aggregatum</i>	Copalchi	LLFS	6SP, 12SP
<i>Moquilea platypus</i>	Sonzapote	FAB	6SP, 12SP
<i>Ocotea puberula</i>	Aguacatillo	FCEA, LLFS	12SP
<i>Persea caerulea</i>	Aguacatillo	LLFS	12SP
<i>Platymiscium curuense</i>	Cristobal	GAM	6SP, 12SP
<i>Quercus insignis</i>	Roble	FCEA, LLFS	6SP, 12SP
<i>Saurauia montana</i>	Moquillo	FCEA	M2, 2SP, 6SP, 12SP
<i>Simarouba amara</i>	Aceituno	LLFS	12SP
<i>Spondias mombin</i>	Jobo	FAB	6SP, 12SP
<i>Sterculia recordiana</i>	Pie de danta	FAB	12SP
<i>Terminalia amazonia</i>	Amarillon	FAB	6SP, 12SP
<i>Theobroma simiarum</i>	Cacao de mono	GAM	12SP
<i>Viburnum costaricanum</i>	Cura	FCEA	6SP, 12SP
<i>Vitex cooperi</i>	Cuajada	FAB	12SP
<i>Zygia longifolia</i>	Zota caballo	FAB, FCEA, LLFS, GAM	6SP*, 12SP

Table S4. Robustness and sensitivity analyses for the richness–dispersion relationship (seven plot-level metrics scaled to unit variance). (A) Permutation test ($n = 9,999$) with standardized effect size (SES). (B) Linear mixed-effects model on betadisper distances along the designed richness gradient (richness fixed, Site/Block random; Satterthwaite df; $N = 96$, M2 excluded). (C) Pairwise betadisper comparisons between all treatment pairs. (D) Leave-one-site-out sensitivity, testing whether the correlation depends on any single site. (E) Replanting sensitivity, excluding replanted individuals (8.1% of trees) and comparing Height Gini ANOVA and betadisper trend with and without replants. (F) Temporal dispersion trajectory (years 2-3) at the three sites with complete temporal data (FAB, FCEA, LLFS), using height and height Gini only. (G) Among- versus within-site variance partitioning of the seven scaled outcomes along the designed richness gradient (M1, 2SP, 6SP, 12SP; M2 excluded). This mean-based variance partition is complementary to the Fig. 4 betadisper dispersion (which uses the spatial-median centroid).

A. Permutation test (9,999 permutations)

Test	Value
Spearman rho	-0.4139
Permutation-p (one-tailed)	< 0.001
SES	-4.03

B. Linear mixed-effects model on betadisper distances

Term	β	SE	df	t	p-value
(Intercept)	2.204	0.205	4.62	10.75	< 0.001
Richness	-0.061	0.017	71	-3.53	< 0.001

C. Pairwise betadisper

Pair	Distance 1	Distance 2	Difference	P-value
M1-M2	2.513	1.724	0.788	0.003
M1-2SP	2.513	1.738	0.775	0.001
M1-6SP	2.513	1.735	0.778	0.004
M1-12SP	2.513	1.551	0.962	0.001
M2-2SP	1.724	1.738	-0.014	0.958
M2-6SP	1.724	1.735	-0.01	0.975
M2-12SP	1.724	1.551	0.173	0.498
2SP-6SP	1.738	1.735	0.003	0.985
2SP-12SP	1.738	1.551	0.187	0.400
6SP-12SP	1.735	1.551	0.184	0.468

D. Leave-one-site-out sensitivity

Dropped	N plots	rho	p-value
None (full)	96	-0.414	< 0.001
FAB	72	-0.478	< 0.001
FCEA	72	-0.332	0.004
GAM	72	-0.35	0.003
LLFS	72	-0.3	0.010

E. Replanting sensitivity

Analysis	Dataset	N trees	N replants excluded	F / rho	p-value	$\eta^2 p$ / M1 dispersion	12SP dispersion
Height Gini	With replants	5760	0	200.7	< 0.001	0.909	NA
Height Gini	Without replants	5291	469	199	< 0.001	0.909	NA
Betadisper	With replants	5760	0	-0.414	< 0.001	2.51	1.55
Betadisper	Without replants	5291	469	-0.373	< 0.001	2.59	1.68

F. Temporal dispersion trajectory (years 2-3)

Year	N plots	rho	p-value	M1	2SP dispersion	6SP dispersion	12SP dispersion
2	72	-0.203	0.0878	1.227	0.731	0.698	0.83
3	72	-0.38	0.001	1.14	0.743	0.726	0.565

G. Among- versus within-site partition of multivariate dispersion

Treatment	n plots	Total SS	Among-site SS	Within-site SS	Among-site %	Within-site %
M1	24	162.6	81.1	81.6	50	50
2SP	24	87.4	26.9	60.5	31	69
6SP	24	92.1	44.1	47.9	48	52
12SP	24	84.4	24.3	60.1	29	71

Table S5. Robustness of the cross-site multivariate-dispersion result to standardization, and underlying mean-variance structure. (A) Spearman ρ between planted richness and dispersion under alternative standardizations/subsets; (B) per-metric mean-variance coupling (Taylor slope of variance on mean across the 16 site×treatment cells); (C) per-metric distance-to-centroid for monoculture vs 12-species; (D) among-site CV by treatment; (E) mixed model of among-site CV on richness.

A. Spearman ρ across standardizations

Standardization / metric subset	ρ (richness vs dispersion)	p	mean-variance immune
Baseline z-score (as published)	-0.41	<0.001	no
Log of productivity metrics	-0.28	0.005	partial
Rank-transform all metrics	-0.06	0.280	yes
Bounded metrics only (survival + 3 Gini)	-0.41	<0.001	yes
Survival only	-0.52	<0.001	yes

B. Mean-variance coupling (Taylor slope ≈ 2 = constant CV)

Metric	type	Spearman(mean, SD)	Taylor slope
Mean height	unbounded	0.81	2.92
Carbon	unbounded	0.94	1.99
Canopy cover	unbounded	0.36	0.88
Height Gini	bounded	-0.23	-0.56
Canopy Gini	bounded	0.19	0.43
Carbon Gini	bounded	-0.01	0.36
Survival	bounded	-0.60	1.19

C. Per-metric dispersion, M1 vs 12-species (ratio >1 = monoculture more variable)

Metric	type	M1	12SP	ratio M1/12SP
Mean height	unbounded	0.95	0.32	2.97
Carbon	unbounded	1.08	0.4	2.72
Canopy cover	unbounded	0.71	0.47	1.51
Height Gini	bounded	0.40	0.29	1.36
Canopy Gini	bounded	0.61	0.59	1.04
Carbon Gini	bounded	0.34	0.64	0.53
Survival	bounded	1.46	0.52	2.82

D. Among-site CV by treatment (%)

Treatment	height	carbon	canopy	ht Gini	canopy Gini	carbon Gini	survival
M1	33	80	36	35	109	16	29
2SP	34	107	74	21	55	17	9
6SP	35	124	72	16	59	9	11
12SP	28	122	80	11	40	23	11

E. Among-site CV ~ richness (LMM, metric random effect)

Metric set	β	p
All 7 metrics	0.002	0.8
Unbounded (productivity)	0.021	0.11
Bounded (survival + structure)	-0.012	0.076

Table S6. Functional diversity saturates along the richness gradient. Presence-based design FD per treatment (mean across four sites; per-site and complete-case values).

Treatment	species richness	Rao's Q (mean \pm SD)	FDis
M1/M2	1	0	0
2SP	2	0.035 \pm 0.017	0.183
6SP	6	0.070 \pm 0.011	0.256
12SP	12	0.073 \pm 0.005	0.262

Table S7. Survival reliability and below-threshold risk by treatment. (A) Mean survival, among-site standard deviation and coefficient of variation (CV), and worst-site survival for each treatment. (B) Modeled probability that a plot falls below the 70% and 80% survival thresholds, with the odds ratio per added planted species (binomial GLMM).

(A) Survival across sites

Treatment	mean survival	among-site SD	among-site CV	worst site
M1	0.78	0.25	0.32	0.56
2SP	0.92	0.06	0.06	0.88
6SP	0.9	0.07	0.08	0.83
12SP	0.9	0.08	0.09	0.8

(B) Probability a stand falls below a survival threshold

Threshold	OR per species (95% CI)	p	P(<threshold) - monoculture	P(<threshold) - 12SP
survival < 70%	0.80 (0.66-0.97)	0.023	0.23	0.025
survival < 80%	0.86 (0.75-0.99)	0.033	0.31	0.076

Table S8. Standardized path coefficients (β) from piecewise structural equation models. Main model uses log-transformed species richness as the predictor (M2 excluded; Fisher's C = 8.55, p = 0.20). The *Inga* proportion model is a robustness check using the proportion of *Inga edulis* per plot (collinear with richness; all treatments included); its coefficients mirror the main model with reversed sign. Site included as a random effect in both models. SE = standard error of the standardized estimate.

Response	Predictor	β	SE	p-value	Model
Height Gini	Log richness	0.83	0.05	< 0.001	Main
Carbon	Log richness	-0.35	0.08	< 0.001	Main
Canopy cover	Log richness	-0.29	0.11	0.007	Main
Canopy cover	Height Gini	0.03	0.11	0.796	Main
Canopy cover	Carbon	0.68	0.07	< 0.001	Main
Canopy Gini	Log richness	0.08	0.06	0.193	Main
Canopy Gini	Canopy cover	-0.81	0.06	< 0.001	Main
Height Gini	<i>Inga</i> proportion	-0.57	0.08	< 0.001	<i>Inga</i> proportion
Carbon	<i>Inga</i> proportion	0.48	0.07	< 0.001	<i>Inga</i> proportion
Canopy cover	<i>Inga</i> proportion	0.31	0.07	< 0.001	<i>Inga</i> proportion
Canopy cover	Height Gini	0.04	0.06	0.508	<i>Inga</i> proportion
Canopy cover	Carbon	0.65	0.06	< 0.001	<i>Inga</i> proportion
Canopy Gini	<i>Inga</i> proportion	-0.07	0.06	0.27	<i>Inga</i> proportion
Canopy Gini	Canopy cover	-0.82	0.06	< 0.001	<i>Inga</i> proportion